Analysis of the effects of Gold nanoparticles on the functional integrity of select serum proteins and heat shock proteins of mammalian origin

By

Duncan Sifiso Luthuli

(20050104)

Dissertation submitted to the Department of Biochemistry and Microbiology in the Faculty of Science and Agriculture, University of Zululand in fulfillment of the requirements for the Master (Msc) degree in Biochemistry.

Supervisor: Dr. A. Shonhai

Co – supervisor: Prof .N. Revaprasadu

February 2012

Abstract

Gold nanoparticles (AuNPs) are a natural starting point for understanding nanoparticle - protein interaction due to their possible applications in biomedical functions, such as disease diagnosis and drug delivery. This has driven interest to understand the effects of AuNPs on the functional and structural integrity of heat shock proteins (Hsp) and serum proteins. When AuNPs are used for medical purposes through the intravenous route, they may be modified by serum proteins and these modifications may give rise to pathologies, or alter the intended purpose of the nanoparticle. Furthermore, Hsp are ubiquitous proteins that occur in cells and are upregulated under stress. It is envisaged that Hsp may also interact with AuNPs delivered to cells and/or the blood circulatory system. In this study, I sought to analyse the interaction between AuNPs and bovine serum albumin (BSA), citrate synthase (CS), malate dehydrogenase (MDH) as well as human heat shock protein 70 (Hhsp70). AuNPs were synthesised by a citrate reduction method in the presence of cysteine as the capping agent, and analysed using UV/visible spectroscopy and transmission electron microscopy (TEM). The effects of AuNPs on the stability of BSA, MDH, Hhsp70 and CS to heat stress were assessed spectroscopically, both in the presence and absence of AuNPs. I further investigated the effects of AuNPs on the function of Hhsp70 in suppressing the aggregation of MDH. Data observed in this study suggested that, the interaction between AuNPs and proteins (BSA and Hhsp70) may be facilitated by sulfhydryl (SH) groups present in them. It was also observed that AuNPs have capabilities of suppressing heat induced aggregation of MDH and CS. Thus AuNPs have chaperone activity as they are capable of maintaining proteins in their soluble, functional forms during heat stress.

Dedication

This dissertation is dedicated to my family.

Declaration

I declare that this is my own, unaided work. It is being submitted for the degree of Master of Science in Biochemistry at the University of Zululand. It has not been submitted for any degree or examination in any other University. All sources have been duly acknowledged.

This _____day of_____2011

Acknowledgements

First and foremost I would like to thank the Lord Almighty for carrying me this far, for without him none of this would have been possible.

I would like to thank my supervisor, Dr. Addmore Shonhai, for being my supervisor, my father and a friend. I also wish to acknowledge in a special way my co-supervisor Prof. Nerish Revaprasadu for his guidance and supervision.

I would like to express my gratitude to Dr. M.M Chili for his research tactics support and Dr Raja for his TEM imaging contribution. Gratitude also goes to the University of Kwazulu-Natal (UKZN) for TEM device, University of Zululand Department of Chemistry (nanotechnology research group) for their unconditional love and support and the Department of Biochemistry (molecular biology research group) for unconditional love and support. I would also like to thank the Department of Science & Technology and National Research Foundation (NRF) of South Africa for providing equipment grant and financial support that made this work possible and the University of Zululand Research Committee for research financing my research study. Lastly, I wish to thank my family and friends for their love and support.

Table of Contents

Table of Figures

List of Tables

List of symbols

Symbol	**interpretation**
β	beta
α	alpha
w/v	weight per volume
th	tenth
pH	*potenz* power + hydrogen
^{o}C	degree Celsius
nM	nanometer (10^{-9} meters)
mol/l	moles per liter
mM	milimolar
ml	milliliter
mins	minutes

mg	milligram
m^{-1}	per meter
M	molar
Kda	kilodalton
g	gram
dl	deciliter
da	dalton
CM^{-1}	per centimeter
a.u	arbitrary units
µM	micromolar
µl	micro liter
≥	Greater or equal
±	Plus or minus
<	Less than
~	Approximately
%	Percent

List of abbreviations

ATP	Adenosine triphosphate
$AuCl_3$	Gold (III) chloride
AuNPs	Gold nanoparticles
B.C	Before Christ
BSA	Bovine serum albumin

$C_6H_5Na_3O_7$	Trisodium citrate
Ca^{2+}	Calcium
Core d	Core diameter
CS	Citrate synthase
C-terminal	Carbon terminal
dH_2O	Deionized water
DNA	Deoxyribonucleic acid
EGFR	Epidermal growth factor receptor
EPR	Enhance permeability and retention
FRET	Forster resonance energy transfer
FTIR	Fourier transform infrared
$HAuCl_4$	Hydrogen tetracloroarate
Hhsp70	Human heat shock protein 70kda
HQ	Hydroquinone
HSC3	Human oral squamous cells carcinoma
Hsp	Heat shock protein
Hsp110	Heat shock protein 110kda
Hsp40	Heat shock protein 40kda
Hsp60	Heat shock protein 60kda
Hsp70	Heat shock protein 70kda
Hsp90	Heat shock protein 90kda
IHRP	Inter α trpsin inhibitor family heavy chain related proteins
K^+	Potassium

MDH	Malate dehydrogenase
MRI	Magnetic resonance imaging
$NaBH_4$	Sodium borohydrite
NaCl	Sodium chloride
N-terminal	Nitrogen terminal
PVP	Poly vinyl pyrrolidone
RNA	Ribonucleic acid
SDS-PAGE	Sodium dodecyl – polyacrylamide gel electrophoresis
SH	Sulfhydryl
sHsp	Small heat shock protein
SLN	Solid lipid nanoparticles
TEM	Transmission electron microscope
UV/vis	Ultra violent/visible

List of research outputs

Publication

Luthuli, D.S., Chili, M.M., Revaprasadu, N., and Shonhai, A. (2012) Analysis of the effect of Gold nanoparticles on the functional integrity of serum proteins and heat shock proteins of mammalian origin. (manuscript in preparation for publication).

International Conference Proceedings

Luthuli, D.S., Shonhai, A., and Revaprasadu, N. Analysis of the effect of Gold nanoparticles on the functional integrity of serum proteins and heat shock proteins of mammalian origin. Biochemistry and Molecular Biology Society of Zimbabwe conference, Zimbabwe (Harare), October 2011.

Local Conference Proceedings

Luthuli, D.S., Shonhai, A., and Revaprasadu, N. Interaction of synthetic gold nanoparticles with select proteins of mammalian origin *in vitro*. SASBMB/FASBMB congress, Drakensberg, South Africa, January 2012.

Chapter 1

Literature review

1. Nanotechnology

1.1 Early history of nanotechnology

Scientific focus on nanosized objects emerged far back in the early 1200 – 1300 B.C. and its recurrence has led to escalating inventions in the field of nanotechnology (Astruc *et al*., 2003). The extraction and appreciation of gold nanoparticles started in the 5th millennium B.C. near Varna (Bulgaria). Interest in this invention multiplied rapidly in Egypt around 1200 -1300 B.C. when the marvelous statue of Tutanichamun was constructed (Astruc *et al*., 2003).

Colloidal gold was historically used to prepare dark red glass, in which gold was present in minimum quantities that were not visible to the human eye. A “Purple of Cassius”, colorant in glasses, was a colloid resulting from the heterocoagulation of gold particles and tin dioxide. This technology was formally appreciated in the 17th century. Further interest in understanding the properties of gold nanoparticles arose in the middle of the 19th century by Michael Faraday (1857), who published work on the preparation and properties of colloidal gold nanoparticles (Turkevich, 1985).

During the last quarter of the 19th century, Faraday’s idea on colloidal gold nanoparticles distended through the development of a method used to prepare hydrosols of metals. This method involved the use of electrodes held close together beneath de-ionised water (arc method) (Bredig, 1988). Zsigmondy (1865-1929) inverted the slit-ultra-

microscope used to visualise colloidal gold properties and Mie gave theoretical explanation for the colour of colloidal gold (Zsigmondy, 1909). After World War one, interest in colloidal gold properties shifted from inorganic systems to high molecular weight organic substances that were both polymers and biochemicals in nature.

Decades ago, interest in metal nanoparticles was limited to applications such as the Damascus steel which was used to make swords and glass Lycurgus cup's which has unique colours (Roco, 1999). After developments of modern devices to analyse nanometer scale material, nano-materials became very attractive as possible machines which can travel through the body. Hence they are able to repair damaged tissues, deliver therapeutic drugs and genes (Andrievskii, 2003).

1.2 Nanotechnology today

Nanotechnology has turned out to be the science of building small structure's and devices that are capable to penetrate body organs, tissues and cells. This technology involves the design, characterisation, production and application of nanosized structures, devices and systems by controlling their shape and size at the nanometer scale. Nanotechnology is envisaged to reach several development levels that will revolutionise materials, devices and systems towards advancing scientific knowledge and technology. Nanotechnology is defined as science which involves particles that are of nanometer size, possessing a large surface area to volume ratio (Fei *et al*., 2009).

1.3 Nanoparticles

Nanoparticles are materials at nanoscale with dimensions about 100 nm or less, they are small enough that they can access almost every part of the human body and some of them have access to the blood brain barrier (Chopra *et al*., 2008). Their surface and size can be manipulated for specific purpose (Jahanshahi *et al*., 2008). Nanoparticles were studied because of their size, shape, physical and chemical properties in ancient times, but today much interest and great concerns are in their biomedical applications (Cedervall *et al*., 2008).

Nanoparticles possess significant adsorption capacities due to their relatively large surface area. This feature allows them to bind and/or carry other molecules such as chemical compounds, drugs, probes and protein attached to the surface by covalent bonds or by adsorption (Heegaard *et al*., 2007). Nanoparticles are useful in biomedicine because of their physiochemical properties such as charge and hydrophobicity (Crombez *et al*., 2008). Nanoparticles that are used as drug delivery vehicles must possess proper delivery capabilities and controlled release properties.

Nanoparticles are generally constituted by two parts, a core material and a surface modifier which together determine their biocompatibility and their physiological fate (biodegradability) (Jong *et al.*, 2008). The core may be made up of biological materials such as peptides, lipids or acids or may be formed by polymers, carbon or metals (Heegaard *et al*., 2007; Crombaz *et al*., 2008). The surface modifier may be employed

to change the physiochemical properties of the core material. The surface coat may also reduce the toxicity of nanoparticles (Dobrovolskaia *et al*., 2007).

Metallic nanoparticles exhibit extra-ordinary optical, thermal, chemical, and physical properties that are as a result of several factors such as energy state and surface area (Feldheim *et al*., 2002). Nanoparticles have also attracted remarkable interest because of their potential applications in catalysis, micro-electronics, electronic and magnetic devices (Zhu *et al*., 2000).

Metal nanoparticles are synthesised in many forms such as nanorods, nanowires, nanotubes and shaped-controlled nanocrystals. Several methods are used in the synthesis of these nanoparticles and include, chemical vapour deposition (Tang *et al*., 2004), electrochemical deposition (Xiao *et al*., 2004), solution-phase reduction, biomolecules-assisted synthesis (Lu *et al*., 2004) and sono-electrochemical methods (Zhu *et al*., 2000). Amongst these, solution-phase reduction method is the most effective method in controlling the size of the product.

1.4 Major classes of nanoscale structures

Major classes of biologically relevant nanostructures include, semiconductors quantum dots, magnetic nanoparticles, polymeric particles, carbon-based nanostructures and metallic nanoparticles.

Nanocrystalline semiconductors (quantum dots) are useful in biological labelling and detection due to their size-dependent fluorescence properties (Brunchez *et al*., 1998). Magnetic nanoparticles find applications in cell sorting (Ito *et al*., 2005), magnetic resonance imaging (MRI) (Josephson *et al*., 2006), drug delivery (Dobson *et al*., 2006) and magnetic hyperthermia therapy (Mornet *et al*., 2004). Lipid and polymeric nanoparticles have been applied in the encapsulation of therapeutic molecules and to increase drug solubility, safety and drug delivery efficiency, as they exhibit enhanced permeability and retention (EPR) effects in tumour tissue (Sershen *et al*., 2002). Carbon-based nanoparticles, especially carbon nanotubes have found increasing interest in biomedical applications, such as photothermal therapy (Shi *et al*., 2005) and drug delivery (Bianco *et al*., 2005).

Metallic nanoparticles have proven to be the most flexible nanostructures owing to their synthetic controllable size, shape, composition, structure, assemblage and encapsulation, as well as the resulting tenability of their optical properties. Compared with other nanoparticles, metallic nanoparticles are more useful in biomedical applications. Colloidal gold nanoparticles hold better promises owing to their simple and easy methods of synthesis and bio-conjugation (Loo *et al*., 2005).

1.5 Synthesis of metallic nanoparticles

Chemical reduction is the most frequently used method for the synthesis of metal colloidal solutions. Gold colloids synthesised by hydrogen tetracloroaurate ($HAuCl_4$) reduction method exemplify synthesis of metallic nanoparticles (Link 1998; Kamat

1999). A number of compounds, both aqueous and organic, including sodium borohydrite ($NaBH_4$) and trisodium citrate ($C_6H_5Na_3O_7$) had been used as common reducing agents.

Colloids produced by the chemical methods are sometimes contaminated with the residual by-products such as metals and reducing agents. The purification of colloid of gold from the by-products is still challenging. Therefore, a laser ablation method had been developed to prepare metal nanoparticles in solutions by the use of laser equipment with various features (Liang *et al*., 2004). The advantages of this method include the relative simplicity of the procedure and the absence of contaminants in the final products. Nanoparticles synthesised by this method are usually of larger scale due to both agglomeration and the possible ejection of the relatively larger target fragments during the laser ablation process.

Metallic nanoparticles can be capped using various shells, such as conductive nonmetallic graphite (Cassagneau *et al*., 1999). This capping can be done *in situ* if the reductive formation of nanoparticles is performed in the presence of the shell-forming material (Cassagneau *et al*., 1999). The shell can also be prepared later through a chemical reaction on the surface of the nanoparticles (Kamat *et al*., 1997).

1.6 Gold nanoparticles (AuNPs)

Gold nanoparticles (AuNPs) are a natural starting point for understanding nanoparticle-protein interaction due to their prospects in diverse biomedical applications, including

their application in many biodiagnostic kits (Gobin *et al*., 2007). AuNPs possess a high extinction co-efficient in the visible region. This extra-ordinary optical feature makes AuNPs an ideal colour reporting group for signaling molecular recognition events and renders them to function as efficient quenchers for most fluorophores (Guan *et al*., 2008). AuNPs typically have dimensions ranging from 1-100 nM and they display distinctive, valuable electric and optical properties. They have different colours determined by their sizes (Winter, 2007) and the deep purple colour of AuNPs is explained by a theory called surface plasmonics resonance (SPR) (Kreibig *et al*., 1995).

1.7 Biomedical applications of gold nanoparticles

Nanoparticles conjugates stimulate (Lucarelli, 2004) or suppress (Ryan, 2007) immunity, and their effect on the immune system is closely influenced by their surface structure. Biomedical applications of AuNPs such as in drug delivery, gene delivery and targeting infected sites allow for controlled delivery and deposition of chemotherapeutic agents to diseased sites. This capability is facilitated by attaching the drugs to nanoparticles and this technique allows the use of lower doses of drugs which are less toxic with improved therapeutic efficacy (Brigger *et al*., 2002).

AuNPs are useful also in cellular imaging and in biosensing due to their appropriate surface in accelerating the antibody-antigen recognition that enhances the immuno-assay signals (Nagatani *et al*., 2006). Immuno-chromatographic assay applications which are frequently used in pregnancy and influenza tests use AuNPs as colour indicators of antibody - antigen reaction (Chio *et al*., 2004).

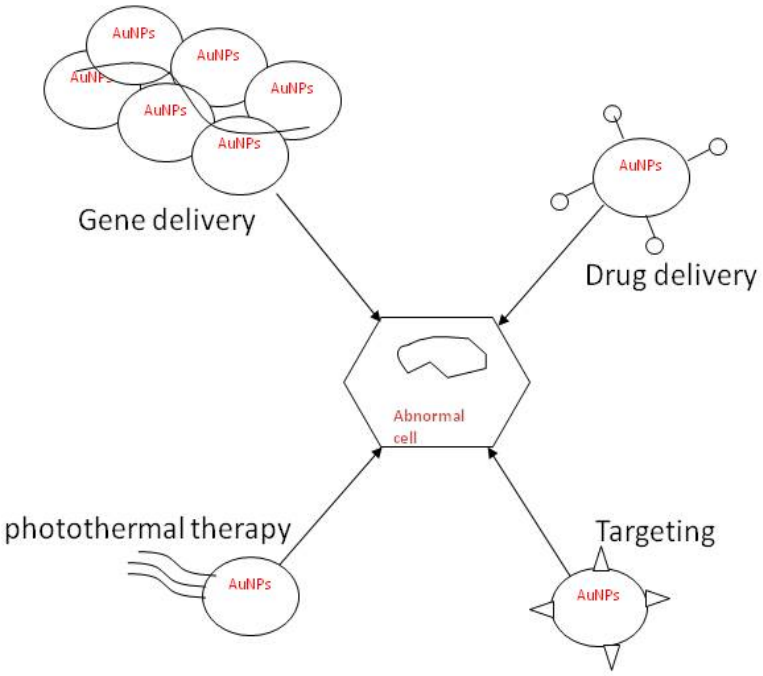

Figure 1.1: Biomedical applications of gold nanoparticles
Diagrammatic presentation of various biomedical applications of gold nanoparticles, AuNPs are employed in delivering genes to specific biologic sites, in delivering chemotherapeutic drug to specific organs, tissues and cells, AuNPs coated with ligands are used to target abnormal cells and AuNPs may be utilized in photothermal therapy (adopted from Gosh *et al*., 2008).

1.7.1 Application of gold nanoparticles for Gene therapy

The key factor to gene therapy application is the lack of safety and effective delivery system (Thomas *et al*., 2003; Park *et al*., 2006). AuNPs compounds exert a number of effects on the immune response, one of them being the reduction in cytokine levels (Fricker, 1996).

Barriers that had been reported to border gene therapy include cellular barrier such as intracellular uptake, endosomal escape, DNA release and nuclear uptake. Intracellular barriers had also been reported. These include avoidance of particle clearance

mechanism, targeting specific tissues and protection of DNA from degradation (Pack *et al*., 2005; Putnam, 2006).

To surmount these downsides, advances had been made to increase nanoparticles efficiency but nonetheless this application is challenged by the electrostatic interaction between positively charged nanoparticles and negatively charged serum proteins (Alexis *et al*., 2008). And also the interaction of gold with thiol groups on the surface of proteins responsible for transcription regulation of the genes that control cytokine expression (Fricker, 1996).

1.7.2 Application of gold nanoparticles in drug delivery

The main advantage of drug delivery using nanoparticles is that, they target pathophysiological sites, avoiding unnecessary influence on healthy tissues (Sahoo *et al*., 2007; Prato *et al.,* 2008). The unique properties of nanoparticles have enabled them to deliver drugs to hard-to-target and/or extremely sensitive sites such as the brain which offers a challenge due to the presence of the blood – brain barrier (Rawat *et al*., 2006; Sahoo *et al*., 2007).

1.7.3 Application of gold nanoparticles in photothermal therapy

AuNPs optical features are useful in therapeutic applications (Jain *et al*., 2007). AuNPs promotes local heating when they are irradiated with light in the “water window” absorption wavelength range (800 nM - 1200 nM). El-Sayed et al (2006), reported work on the application of AuNPs coated with anti-EGFR (Epidermal growth factor receptor)

to target HSC3 (Human oral squamous cell carcinoma) cancer cells in photothermal destruction of tumors cells (Haung *et al*., 2007). The outcomes of his study concluded that the use of AuNPs enhanced the efficiency of photothermal therapy by twenty times.

1.7.4 The use of nanoparticles in disease diagnosis and research

Radio-active or organic fluorophore labelling of the probe molecule techniques had been linked with the use of DNA chips as a requirement for the need for comparability in combination with decrease of sample volume in DNA detection.

AuNPs had been used to signal hybridisation in most deoxyribonucleic acid/ribonucleic acid (DNA/RNA) assays using either one of the three known strategies for detecting gold tracers. These strategies include, direct detection of the nanoparticle on the bare electrode without dissolving the particle (Ozsos *et al*., 2003), the direct electrochemical oxidation of the particle using the electrochemical signal of the dissolved particle (Wang *et al*., 2001), and the use of silver deposited on AuNPs to enhance electrochemical signal (Wang *et al*., 2002).

The molecular basis of nanoparticles based DNA/RNA bio-detection methods rely on efficient cross-linking mechanism of gold nanoparticles with homogenous DNA/RNA. This method was first described by Mirkin et al (1996); Mirkin used thiol-linked oligonucleotide modified AuNPs for the colorimetric detention of DNA targets. Sato *et al* (2003) detected mismatched oligonucleotide by increasing salt concentration which resulted in induced aggregation of oligonucleotide-functionalised AuNPs using non

cross-linking mechanism. The induced aggregation was signified by the colour of AuNPs changing from red to deep purple. However, nucleic acids sequences protected AuNPs from aggregating, possibly through electrostatic interaction between the negatively charged phosphate groups of the nuclei acid and the highly polarisable gold nanoparticles (Sandstrom *et al*., 2003).

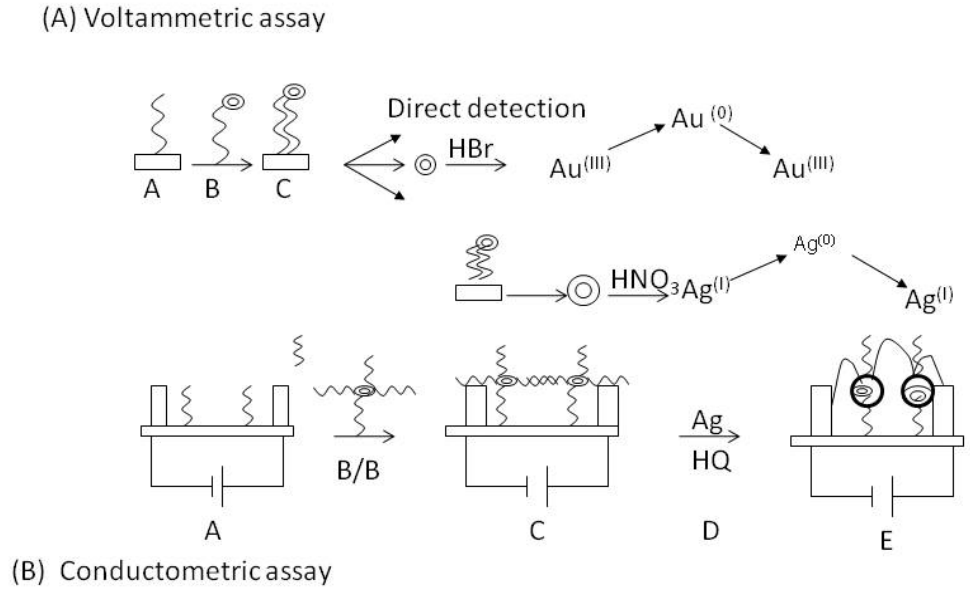

Figure1.2 Detection strategies of gold nanoparticles
(A) Potentiometric/voltammetric stripping assay. The hybridization event occurs between DNA strand (A) and gold-tagged DNA (B). The gold-labeled duplex (C) formed is then detected according to each strategy: (i) direct detection of the nanoparticles onto the bare electrode without the need for tag dissolution; (ii) the gold nanoparticles are dissolved with HBr/Br_2 treatment and then detected by stripping techniques; and, (iii) The gold nanoparticles are first covered with Ag by a deposition treatment and then detected by stripping techniques via silver enhanced signal. (B). Conductivity assay. Probe DNA immobilised in a small gap between two electrodes (A) is hybridised with target DNA (B) and then with gold-modified DNA probes (B/B). Gold is accumulated in the gap (C). Silver enhancement (D) is performed in the presence of hydroquinone (HQ). The silver precipitated onto the gold nanoparticles (E) improves the sensitivity of the assay by lowering the resistance across the electrode gap. Picture adopted from (Merkoci *et al*., 2005).

1.7.5 Application of gold nanoparticles in tissue engineering

Osteoblasts are the cells responsible for the growth of the bone matrix and are found on the advancing surface of the developing bone. Natural bone surface contains features

that are about 100 nM across. If the surface of the artificial bone implant is left smooth, the body would try to reject it. Due to this, smooth surfaces may develop fibrous tissue that eventually covers the surface of the implant (Gutwein *et al*., 2003). This layer reduces the bone - implant and further inflammation results in loosening of the implant. The creation of nanomaterials features on the surface of the hip or knee prosthesis reduces chances of tissue rejection and stimulates production of osteoblast tissues (Gutwein *et al*., 2003).

1.8 Proteins

Proteins are important biomolecules. They are built up of 20 different amino acids, and larger numbers of proteins are polymerised to long chains referred to as polypeptides. After their synthesis, they fold up into three dimensional compact shapes (native protein) determined by a particular amino acid sequence (Elliot *et al*., 2005).

Proteins occur in various structural forms such as hormones, enzymes, haemoglobins, antibodies, membranes and structural proteins. Their conformation can be modified by environmental conditions such as the binding of metals or small molecules, chemical modifications or by exposure to temperature, light, pressure and other physical agents (Bray, 2005). Conformational changes of proteins, which result from the intrinsic flexibility of their structures, may occur due to their modification by nanoparticles (Chah *et al*., 2006).

Proteins are never regarded as firmly stable due to the counter balance of energy loss related with changing from the larger ensemble state to the more restricted set of conformation, and this interplay defines their native state. In addition, the repulsive electrostatic interactions present in the native state, result in the reduction of their stability (Lynch *et al*., 2008).

1.8.1 Interaction of nanoparticles with proteins

Binding of proteins to planar surfaces often induces significant changes in the secondary structure. The high curvature of nanoparticles can help proteins to retain their original structure and nanoparticles of large size have low surface curvature, while those of small size possess high surface curvature. The curvature is lowest for planar surfaces (Fei *et al*., 2009). Research on nanoparticle surfaces and proteins indicate that the perturbation of protein structure happens at varying extents when proteins are absorbed to nanoparticles.

Bovine serum albumin (BSA) is a well-studied protein which readily undergoes conformational changes in response to physiological changes such as pH. Hence, BSA provides a good model for investigating the effect of nanoparticles on protein conformational change. Shang *et al* (2007) reported that, in the presence of AuNPs, BSA shows a decline in α-helical structure and a significant increase in β-sheet content (Shang *et al*., 2007).

1.8.2 Effects of nanoparticles on protein structure and function

As nanoparticles become smaller; their surface areas shrink more slowly than their volumes, causing them to have far greater surface-to-volume ratios. A larger surface-to-volume ratio also implies that more proteins will bind to a nanoparticle (relative to its mass) than a particle of larger size. Even for larger particles, protein binding is established as one of the most important factors influencing biodistribution (Cedervall *et al*., 2007). A systematic study of the effect of nanoparticle size on the structure and function of adsorbed proteins has been performed, in which lysozyme was adsorbed onto silica nanoparticle (Vertegel *et al*., 2004).

1.8.3 The nanoparticle – protein corona

The effective unit in cell-nanoparticle is believed to be the nanoparticle and its corona or more or less associated serum proteins or other body fluid but not the nanoparticle as such (Lynch *et al*., 2006). Composition and organisation of this protein layer is not the only important procedure, the exchange times between the nanoparticle and the protein that the cell reacts with is also important (Lynch e*t al*., 2008).

Proteins associated with a particle possess wide range of affinities in the particle surface, resulting in a range of different residence times for a protein at a nanoparticle surface. The composition of a protein corona at any given time will be determined by the concentrations of over 3700 proteins in plasma (Muthusamy *et al*., 2005).

1.8.4 Kinetics of nanoparticles – proteins interaction

The composition of the nanoparticle-protein corona at any given time relies on the concentrations and kinetic properties of serum proteins. Therefore, it is important not only to determine which proteins are adsorbed onto the surface of the nanoparticle, but also to understand the binding affinities (k_d) and stoichiometries. Protein affinities on the nanoparticle surface differ from their affinities to analogous bulk materials due to a variety of effects including size, surface area, and the curvature of the nanoparticle surface (Kim *et al*., 2007).

The continuation of the nanoparticle-protein complex is sustainable for the duration of the nanoparticle's stay in the body. It is possible that those proteins in high concentrations in plasma and with high association rates will initially occupy the surface of the nanoparticle. However, over time, these proteins may dissociate and be replaced by proteins of lower concentrations depending on the prevailing thermodynamics (Cedervall *et al*., 2007).

The process of competitive adsorption of proteins onto a limited surface based on abundance, affinities, and incubation time is collectively known as the "Vroman Effect" (Vroman *et al*., 1980). This effect is important to consider with regards to distribution of nanoparticles throughout the body. As nanoparticles are distributed from the blood to various locations, the differences in protein levels, as well as their affinities for binding, may play an important role in determining how the protein corona evolves.

Previous kinetic studies on solid lipid nanoparticles (SLN) showed that initial protein binding was predominated by albumin, and replaced over time by fibrinogen which was then replaced by IHRP (inter-α- trypsin inhibitor family heavy chain-related protein) and apolipoproteins (Blunk *et al*., 1993). Also shown was that with increasing plasma concentrations, the amount of fibrinogen on the SLN surface decreased while the amount of apolipoproteins steadily increased (Harnisch *et al*., 2000). Even though the concentrations of the several apolipoproteins found in human plasma are substantially lower than that of fibrinogen, the affinity of apolipoproteins especially to hydrophobic surfaces is much higher (Gopper *et al*., 2005).

Although the protein may retain most of its native structure after adsorption on the nanoparticle surface, in some cases the thermodynamic stability of the protein is decreased. This makes the protein to be more sensitive to chemical denaturants such as urea (Shang *et al*., 2007). Hence, concerns have been raised about the application of protein- nanoparticle conjugates, as changes in protein structure or stability may lead to loss of biological function.

Therefore, it is essential to understand in detail the effects of protein-nanoparticle adsorption, including identifying which properties of nanoparticles determine their tendency to perturb protein conformation. In general, structural changes occur due to the intrinsic properties of the protein combined with features of the nanoparticles, such as surface chemistry and surface curvature. In addition, recent studies have

characterised how the effect of protein concentration at the nanoparticle surface influences effects on protein structure and function (Wu *et al*., 2008).

1.9 Serum albumin

Bovine and human albumins are free carbohydrate proteins composed of three homologous domains (Sugio *et al*., 1999). Human albumin has a molecular mass of 66, 430 dalton (da) and bovine albumin has a molecular mass of 66, 267 da, and the two proteins share approximately 80% homology. Bovine albumin is composed of 582 amino acids residues and human albumin is composed of 585 amino acids residues. Each albumin molecule consists of nitrogen concentration ranges between 16, 3 - 16, 5% and 35 cysteine residues which may be involved in 17 intramolecular disulfide bridges. These residues may account for the overall conformation and stability of albumin molecules (Peters, 1985). Amongst all 35 residues observed in albumin molecules, the cysteine 34 residue is located at the solvent interface of each albumin molecule and contains a free sulfhydryl (SH) group that is liable to oxidation and form disulfide bonds. The sulfhydryl group is susceptible to oxidation by cysteine or glutathione, resulting in mixed disulfide bonds formation (Frank *et al*., 2010).

Characterisation of the SH of albumin molar ratio and extinction co-efficient depends on the age of an albumin molecule and the method of purification. Serum albumin's function is to bind and transport fatty acids, hormones, metal ions, maintenance of osmotic pressure and pH, and binding of exogenous toxins and products of lipid oxidation (Bertucci *et al*., 2002). Serum proteins also consist of 67% α-helics structures.

Amongst the 3700 plasma proteins which constitute the plasma proteome (Cedervall *et al*., 2005), approximately 50 have been identified in association with various nanoparticles (Kim *et al*., 2007). Serum consists of two 'families' the albumins and the globulins and potentially carries a record of important histological information, whose determination could serve to improve early detection of diseases (Radhakrishna, 2010).

Albumin is mainly made in the liver and prevents the blood from leaking out of blood vessels, and it is used to transport medicines and other substances through the blood and it is also important in tissue growth and healing. Globulin is made up of different proteins called alpha, beta, and gamma types. Some globulins are made by the immune system; some bind with hemoglobin and other transport metals, such as iron in the blood and fight infection.

Table1: Serum proteins
Table showing serum protein composition and their functions (Alper, 1974).

Blood proteins	**Normal levels**	**% abundant**	**Physiological Function**
Albumins	3,5-5 g/dl	≥60	Create oncotic pressure and carrier of other molecules
Immuno-globulins	1,0-1,5 g/dl	18	Participate in immune system
Fibrinogens	0,2-0,45 g/dl	4	Blood coagulation
α 1- antitrypsin			Neutralise trypsin that has leaked from the digestive system
Regulatory protein		<1	Regulation of gene expression

1.10 Toxicity of nanoparticles and heat shock protein expression

Toxicology studies suggest that nanoparticles possibly cause adverse health effects, but the fundamental cause-effect relationship is still yet to be understood. Thus interaction of nanoparticles with physiological materials has become the most recent focus in biomedical research (Nel *et al*., 2006). Nanoparticle diameters are similar to diameters of cellular components and proteins; therefore, they can bypass membranes barriers and cause damages to tissues and cells (Pan *et al*., 2007).

Heat shock proteins (Hsp) are highly conserved, ubiquitous proteins that occur in most life forms, whose main role is to act as molecular chaperones by facilitating protein to refolding to the native state (Ellis, 1987). They recognise, bind and assist other proteins fold to native status (Hendrick, 1993).

Heat shock proteins associate with their substrate for various purposes including keeping the partner proteins in a folding competent state, facilitating localisation and import/export of targeted proteins, reducing the degree of aggregation of non-native proteins and facilitating the degradation of non – native and aggregated proteins (Hofmann 1999).

The major families of heat shock proteins include small heat shock proteins (sHsp), heat shock protein 40 (Hsp40), heat shock protein 60 (Hsp60), heat shock protein 70 (Hsp70), heat shock protein 90 (Hsp90) and heat shock protein 110 (Hsp110). Heat shock proteins have been proposed as cancer drug targets (Calderwood *et al*., 2006).

Some small molecule inhibitors that target heat shock proteins have been presented as potential drugs against disease such as cancer (Calderwood *et al*., 2006).

Heat shock protein 70 (Hsp70) forms one of the major heat shock protein families. Generally Hsp70 proteins are induced in response to stress, although some Hsp70 species are constitutively expressed in cells. Hsp70 binds to peptide substrate, allowing it to refold; followed by release of the substrate in ATP- expending cycles (Szabo *et al*., 1994). Hsp70's high peptide substrate affinity is reduced in the ATP-bound state (Suh *et al*., 1999).

ATP binding induces a structural change that transcends to the peptide-binding domain from the ATPase domain, resulting in the protein attaining low substrate affinity states, leading to release of substrate (Liberek *et al*., 1991). Hsp70 proteins have a molecular weight of approximately 70 kDa and consist of two distinct domains; the 45- kDa N-terminal domain that binds ATP, and the 25-kDa substrate-binding domain (Flaherty *et al*., 1990; Wang *et al*., 1993). Heat shock protein 90 (Hsp90), Hsp70/Hsp40 partnerships and small heat shock proteins are potential antimalarial drug targets (Shonhai, 2010). Hsp 70 provides cardio protection after ischemia-reperfusion injury (Jayakumar, 2001).

1.11 Hypothesis

Despite the outstanding developments associated with nanotechnology, there is insufficient understanding regarding the interaction between nanotechnological objects and biological systems (Cedervall, 2006). Gold nanoparticles present themselves as prospective agents to be used in biomedical applications and in molecular research (Gobin *et al*., 2007).

However, there are fears that gold nanoparticles injected in the blood stream may be modified by serum proteins. These modifications may give rise to pathologies, or alter the intended purpose of the nanoparticles. The properties of the protein coat may ultimately define the biological response to the nanoparticle (Moghimi, 2001).

It is envisaged that heat shock proteins may also interact with gold nanoparticles delivered to cells and/or the blood circulatory system. Given the importance of heat shock proteins to cell survival, it is important to understand how synthetic gold nanoparticles may interact with these proteins.

1.12 Specific objectives of the study

The primary objective of this study was to analyse the interaction between gold nanoparticles (AuNPs) and select serum proteins as well as some heat shock proteins of mammalian origin.

The following specific objectives were pursued in this study:

1. Synthesis and characterisation gold nanoparticles.

2. Investigation of the interaction between gold nanoparticles and human heat shock protein 70 and bovine serum albumin *in vitro*.
3. Investigation of the capability of AuNPs to improve or suppress stability of malate dehydrogenase (MDH) and citrate synthase (CS) under thermal stress.
4. Assessment of the effect of AuNPs on the function of Hhsp70 with respect to its ability to suppress heat-induced aggregation of MDH *in vitro*.
5. Assessment of the solubility status of MDH and CS following heat treatment in the presence of AuNPs.

Chapter 2

Methodology

For all reported work, at least three independent experiments were conducted.

2.1 Synthesis and characterisation of gold nanoparticles

Rationale

This experiment was designed to synthesize gold nanoparticles which were capped with cysteine. It was important to ensure that the particles had the features that are amenable for biological applications such as the possession of an amino acid based surface coating.

2.1.1 Synthesis of gold nanoparticles

The method followed for the synthesis of AuNPs was slightly modified from the protocol first described by Turkevich et al (1951). Firstly, AuNPs were synthesised by reducing gold (III) chloride ($AuCl_3$) 0.05 mM with sodium borohydride ($NaBH_4$) 0.01 mM in the presence of cysteine with varying concentrations (1 mM, 2 mM, 3 mM and 4 mM) as the capping agent. The reactions were allowed to proceed for 2 hours at room temperature, and sampling was done after 30 mins and at the end of the reaction. The products obtained from experiments conducted using the above mentioned reaction parameters were uncharacteristic of AuNPs. Therefore, the synthesis of AuNPs was optimised. To do this, 33 mM cysteine was stirred for 30 mins resulting in a colourless solution. $AuCl_3$ was added to the reaction mix at a final concentration of 0.1 M and a yellow product resulted. $NaBH_4$ was added to the reaction mix at a final concentration of 1 M and the

reaction colour changed to ruby red (red-wine colour). The reactions were allowed to proceed for 2 hours, and sampling was done after 5 mins, 30 mins and at the end of the reaction. The final products were transferred to a sterile centrifuge tube for storage and subsequent analysis.

2.1.3 Characterisation of gold nanoparticles by UV/visible absorption spectroscopy and Transmission Electron Microscopy

UV/visible absorption spectroscopic analyses of AuNPs were carried out using a Perkin Elmer lambda 20 spectrophotometer. Imaging was conducted using Philips CM 120 Biotwin transmission electron microscope (TEM) and the images were viewed and captured on 80K self-imaging system mega-view III digital copper grade (Chili *et al*., 2008).

2.2 Investigation of the interaction between gold nanoparticles and bovine serum albumin (BSA) and human heat shock protein 70 (Hhsp70) *in vitro*

Rationale

AuNPs capped with cysteine may possibly interact with serum proteins in the blood considering that serum albumin possesses 34 cysteine residues which are positioned at the solvent interface of the protein. Albumins possess a free sulfhydryl (SH) group that is prone to mixed disulfide bonds formation (Alexis *et al*., 2008). Previous studies have suggested that amongst 3700 serum proteins, 50 have been associated to interact with various nanoparticles (Kim *et al*., 2007). Hhsp70 may possibly interact with AuNPs

through its sulfhydryl and functional sub-domains such as its ATPase and substrate binding domain.

2.2.1 Analysis of the interaction of AuNPs with BSA and Hhsp70

BSA and Hhsp70 at their final concentrations of 0.01 mg/ml and 0.01 mg/ml respectively, were prepared in 1 ml of phosphate buffer saline (pH 7.4) (PBS; see appendix A for buffer preparation). The mixture was homogenously mixed with AuNPs at a final concentration of 1.086 x 10^{-5} mol/l in a 1 ml quartz cuvette. The solution was left to stand before being subjected to UV/visible spectroscopic analysis (see appendix A, Fig A1). A control experiment involved analysis of the spectra of AuNPs in the absence of protein. Emission spectra were recorded in the 200 nm - 800 nm fluorescent ranges (Li-Mei *et al*., 2006). At least three independent experiments were undertaken.

2.2.2 Validation of the specificity of the interaction between AuNPs and BSA

AuNPs was prepared at a final concentration of 1. 086 x 10^{-5} mol/l and to this BSA was added at varying final concentrations of 0.02, 05, 0.1 mg/ml. The mixture was allowed to equilibrate and a sample was transferred to a 1 ml quartz cuvette for spectroscopic analysis (Horovitz *et al*., 2007). At least three independent experiments were conducted.

2.2.3 Analysis of the Interaction of AuNPs with BSA under different pH conditions

BSA was prepared at a final concentration of 0.1 mg/ml at various pH points (1.6; 4.6; 7.4; 8.0 and 10.5) suspended in PBS (pH 7.4). To this, AuNPs were added to a final

concentration of 1. 086 x 10^{-5} mol/l. The mixture was allowed to equilibrate and samples were transferred to a 1 ml quartz cuvette and analysed using a UV/vis spectroscopy (Li-Mei *et al*., 2006). The excitation wavelength of the protein was measured before the addition of AuNPs and emission spectra were recorded from 200 nm – 800 nm for the fluorescent properties of AuNPs + BSA complex. At least three independent experiments were undertaken.

2.3 The evaluation of the effects of AuNPs on the heat-induced aggregation of human heat shock protein 70 (Hhsp70), malate dehydrogenase (MDH), citrate synthase (CS) and bovine serum albumin (BSA)

Rationale

Hsp 70 is known to interact and suppress aggregation of MDH and CS in the presence of heat stress (Ahrman *et al*., 2007; Shonhai *et al*., 2008). It was curious to investigate the effect of AuNPs on the stability of MDH and CS to heat stress.

2.3.1 Investigating the effect of gold nanoparticles on the stability of MDH, CS, BSA and Hhsp70 against heat stress

Proteins are known to aggregate in response to heat stress. In this section, the stability of MDH, BSA, CS and Hhsp70 in the presence and absence of AuNPs was investigated at 48^{o}C. Firstly, the aggregation of proteins in the absence of AuNPs was investigated as follows; 1 ml of assay buffer (20 mM tris, pH 7.4; 100 mM NaCl) (Ramya *et al*., 2006) (see Appendix A for buffer preparation) was prepared into which the respective proteins

were added in separate tubes to a final concentration of 1.3 µM for BSA and Hhsp70 and 0.65 µM for MDH and CS. The solutions were placed in a quartz cuvette which was positioned on a port at 48^{o}C and protein aggregation was monitored based on the development of turbidity at 360 nm (Bash *et al*., 2004).

Subsequently it was investigated, whether a solution AuNPs would contribute towards turbidity in the absence of protein at this temperature as a control experiment. AuNPs at a final concentration of 1.086 x 10^{-5} mol/l were added to 1 ml of assay buffer. The solution was similarly exposed to 48^{o}C and readings were taken every 5 minutes for 30 minutes. For the rest of the proteins the reactions were allowed to proceeds for 30 minutes, but for CS the reaction was allowed to proceed for 45 minutes.

The effect of AuNPs on the stability of proteins at 48^{o}C was investigated. The reaction was repeated in the presence of respective proteins and AuNPs (1.086 x 10^{-5} mol/l). As a positive control, suppression of MDH aggregation in response to heat stress was investigated in the presence of Hhsp70 as it is a known chaperone (Shonhai *et al*., 2008).

Furthermore, to confirm the possible capability of AuNPs to suppress MDH and CS aggregation in response to heat stress, the reaction was repeated at the following variable concentrations of AuNPs (0.13 x 10^{-5}, 0.54 x 10^{-5}, 0.64 x 10^{-5}, 0.86 x 10^{-5} mol/l).

2.4 Analysis of the solubility status of MDH and CS following heat treatment in the presence and absence of AuNPs

Rationale

The solubility status of proteins is more likely to signify their structural and functional features under heat stress. Normally, proteins tend to aggregate in response to heat stress. Therefore, this study sought to investigate how AuNPs would influence the solubility of proteins subjected to heat stress.

The capability of AuNPs to suppress MDH and CS aggregation was further assessed using a slightly modified protocol by Ahrman et al (2007). In a reaction, 20 µl sample containing 1 µM CS and/or 1 µM MDH was pre-incubated in the presence of AuNPs at a final concentration of 1.086×10^{-5} mol/l, and in the absence of AuNPs, respectively. The reaction mix was incubated at 48°C for 20 mins. To separate soluble protein from the aggregated protein, samples were centrifuged for 10 mins at 14,000 g. A total of 15 µl of the supernatant was removed (soluble protein) and mixed with SDS-PAGE loading buffer (see Appendix A for buffer preparation). The remaining pellet was re-suspended in SDS-PAGE loading buffer. The samples were analysed by SDS-PAGE.

The electrophoresis apparatus was set up with the cathode buffer covering the gel in the negative electrode chamber, and the anode buffer in the lower positive electrode chamber (25 mM Tris, pH 8.3; 250 mM glycine and 0.1 % (w/v) SDS). There after, the boiled sample proteins were added to the wells from one end of the gel with a pipette.

Finally, the apparatus were connected with the electrophoresis voltage set at 120 V for separation of the protein bands. An electric field was applied across the gel, causing the negatively-charged proteins to migrate across the gel towards the anode. Depending on their size, each protein moved differently through the gel matrix (Deyl, 1983).

Chapter 3

Results

3.1 Synthesis of gold nanoparticles

The starting materials used in the synthesis of AuNPs were $AuCl_3$, $NaBH_4$ and cysteine. Their absorption spectrum was individually confirmed using UV/vis spectroscopy (Fig 3.1). It was anticipated that as AuNPs are formed, their characteristic absorption spectrum would be observed as distinct from that of the starting materials.

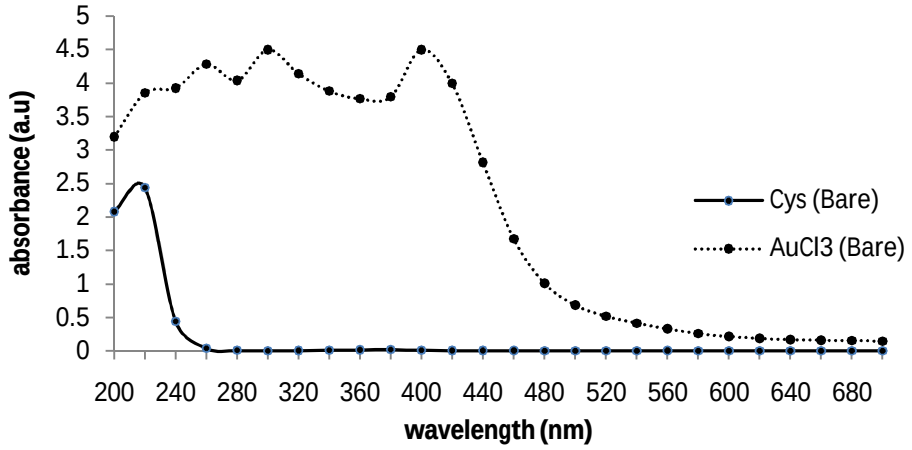

Figure 3.1 UV/vis spectrums of $AuCl_3$ and cysteine
Absorption wavelengths of $AuCl_3$ and cysteine were investigated using UV/visible spectra, analysis were conducted using 1 mM cysteine and 0.01 M $AuCl_3$. Absorbance (a.u) represents arbitrary units and wavelength (nm) represents distance between adjacent peaks in nanometer.

The method used to synthesise AuNPs was based on a protocol by Turkevich et al (1951). In the first approach, the following reagents were used: $AuCl_3$ (0.05 mM), $NaBH_4$ (0.01 mM), cysteine (1 mM, 2 mM, 3 mM, 4 mM). This approach led to the generation of products that exhibited characteristics that were not consistent with AuNPs (Fig 3.2). Apart from an unusual absorption spectrum, the product was colourless, AuNPs are

known to exhibit a ruby red colour (red-wine colour) (Chen *et al*., 2005; Chili *et al*., 2008).

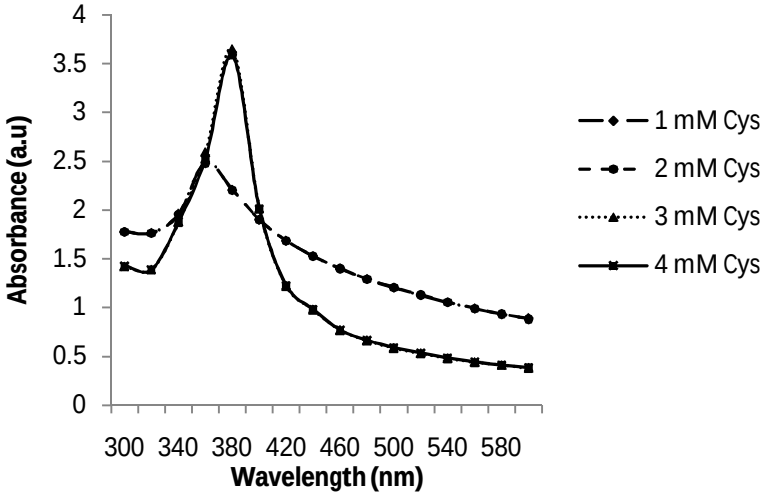

Figure 3.2 UV/vis spectra of AuNPs synthesised with different $AuCl_3$, $NaBH_4$ and cysteine concentrations

AuNPs synthesized by the reduction of 0.05 mM $AuCl_3$ with 0.01 mM $NaBH_4$ and capped with 1, 2, 3 and 4 mM cysteine concentrations for 2 hours of reaction irradiation presented strong UV/vis absorption wavelengths. 1 mM and 2 mM cysteine concentrations presented absorption peaks that were identical and low in intensity at ~369 nm, compared to 3 mM and 4 mM cysteine concentrations that also had identical absorption peaks at ~380 nm and high intensity. Absorbance (a.u) represents arbitrary units and wavelength (nm) represents distance between adjacent peaks in nanometer.

Therefore, the synthesis of AuNPs was repeated to optimise the reaction conditions (refer to, section 2.1.1) in which the following reaction concentrations were used: $AuCl_3$ (0.1 M), $NaBH_4$ (1 M) and cysteine (33 mM). The introduced changes led to the yield of products that had typical characteristics of AuNPs, based on UV/vis spectroscopy (Fig 3.3). AuNPs obtained had their SPR peaks at approximately 370 nm-380 nm. The principle of SPR is based on utilizing the optical features of metallic nanoparticles and can be well performed using the UV/vis spectroscopy. The intention was to produce AuNPs that exhibit features appropriate for biomedical applications (Horovitz *et al*.,

2007). The products obtained following the optimisation of the protocol exhibited features amenable for possible biomedical application.

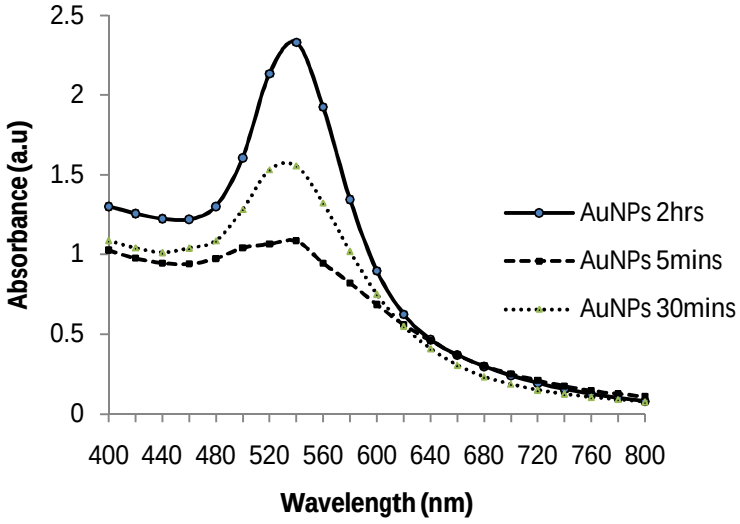

Figure 3.3 UV/vis spectra of gold nanoparticles produced by optimised concentrations of parameters

UV/visible spectral analysis of cysteine capped AuNPs synthesized at various time intervals using 0.1 M $AuCl_3$, 1 M $NaBH_4$ and 33 mM cysteine. Compound black line signifies AuNPs synthesised for 2 hours, middle dotted line signifies AuNPs synthesised for 30 mins and dashed line signifies AuNPs synthesised for 5 mins. Absorbance (a.u) represents arbitrary units and wavelength (nm) represents distance between adjacent peaks in nanometer.

Based on UV/vis spectroscopy, the particles exhibited absorption wavelength peaks at approximately 530 nm. It was noted that, the variation in time of synthesis resulted in slight variations of their absorption wavelength peak (Fig 3.3).

3.1.2 Transmission Electron Microscopy (TEM) of AuNPs

The average diameter and the character of biodistribution of AuNPs are influenced by reaction conditions (Turkevich, 1985). The formation of AuNPs involves interchange of several processes such as the nucleation, growth and coagulation (Turkevich, 1985). The principal function of transmission electron microscope in the synthesis of AuNPs was to confirm size and shape variations of the prepared AuNPs.

TEM analysis of AuNPs synthesised for 30 mins presented AuNPs that were primarily spherical in shape with diameters that ranged between 35 nm – 55 nm. The batch of AuNPs synthesised for 2 hours were dominated by hexagonally shaped AuNPs with diameters range between 25 nm – 45 nm (Fig 3.4). TEM figures are given in the same scales, so the differences in the size of nanoparticles distinct as the crystal lines were more visible in AuNPs synthesised for 30 mins (Fig 3.4).

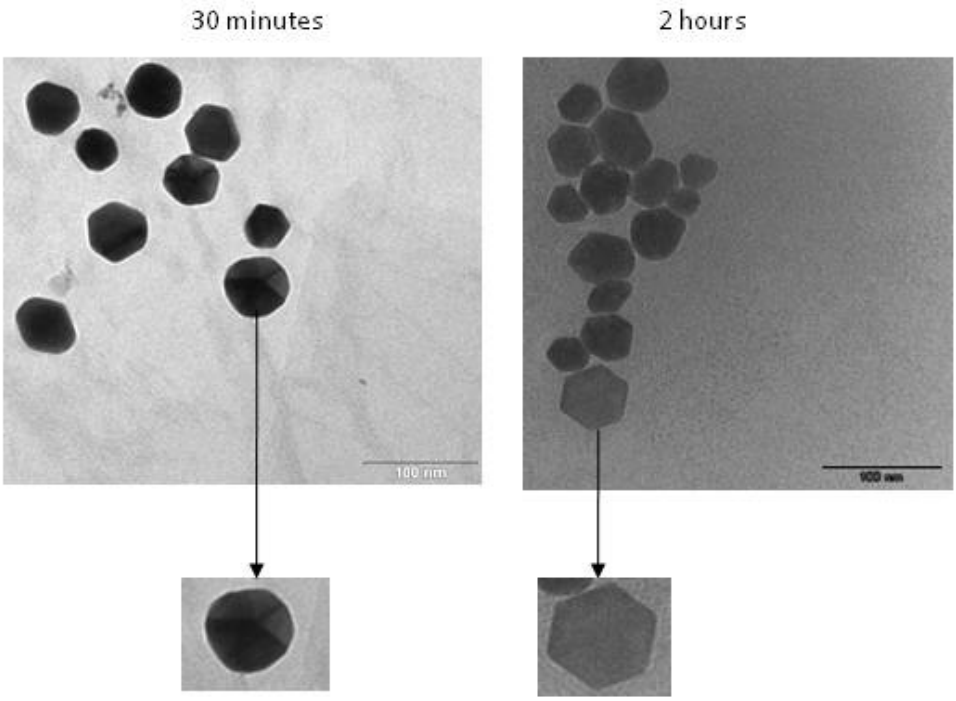

Figure 3.4 Characterisation of AuNPs synthesised for 30 mins and 2 hours respectively
Transmission electron microscopic images of AuNPs, (A) AuNPs synthesised for 30 mins and pulled down image represents a single spherical shaped AuNP, (B) AuNPs synthesised for 2 hours and pulled down image represents a single hexagonally shaped AuNP.

3.2 Interaction of AuNPs with human heat shock protein 70 and bovine serum albumin

The properties of nanoparticles influence their association with proteins and in turn, the properties of particular proteins influence their interaction with a given nanoparticle

(Chithrani *et al*., 2006; Dutta *et al*., 2007). The resultant change in size of nanoparticles as they associate with proteins is known to influence the function of the latter such as their distribution profile in biological systems (Moghimi *et al*., 2001).

BSA (alone), Hhsp70 (alone) and AuNPs (alone) had their UV/vis absorption spectra confirmed (Fig 3.5A). This was done in order to differentiate the absorption spectra of the proteins alone, as compared to that of AuNPs-complex. The possible interaction between AuNPs and BSA and Hhsp70 was investigated at pH 7.4 at a final concentration of 0.01 mg/ml of protein. The observed drop in intensity (arbitrary units) and red-shift in absorption wavelength peaks observed when AuNPs were exposed to proteins signifying possible interaction between AuNPs and BSA and with Hhsp70, respectively (Fig 3.5B). The shift in wavelength also suggests that the apparent size of the nanoparticle increased in the presence of proteins compared to AuNPs alone (Fig 3.5B). Similar observations were made by Horovitz *et al* (2007) who observed that, when proteins interact with AuNPs, the apparent sizes of the particles increase due to absorption of proteins and the resultant changes in the dielectric constant.

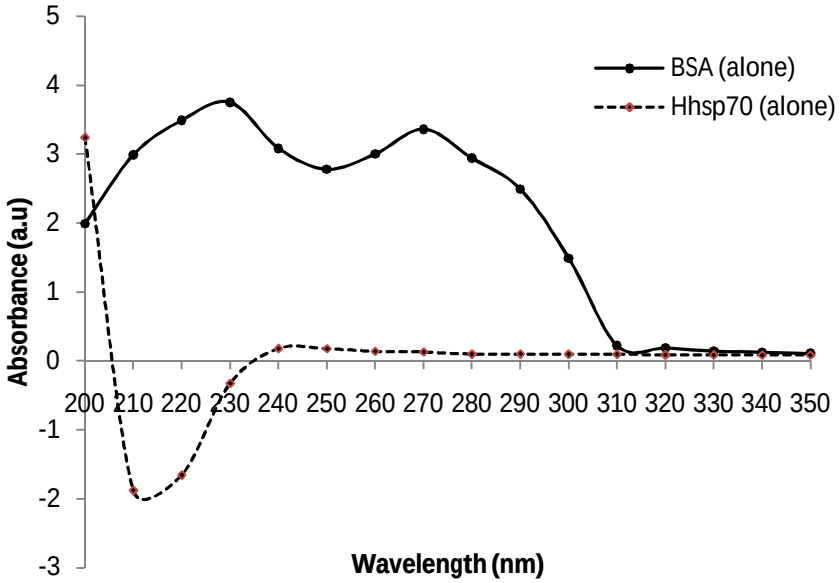

Fig 3.5A The UV/vis absorption spectrum of proteins
BSA (alone) and Hhsp70 (alone) were analysed individually for their wavelength spectrum peaks using UV/vis absorption spectroscopy.

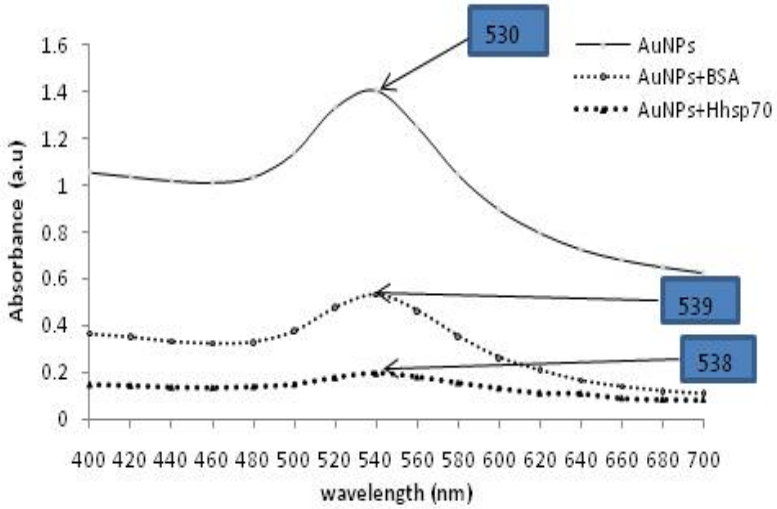

Figure 3.5B Interaction of AuNPs with Hhsp70 and BSA as confirmed by spectrometry
Interaction of 1.086 x 10^{-5} mol/l AuNPs with 0.01 mg/ml Hhsp70 and 0.01 mg/ml BSA *in vitro* as presented by UV/vis spectroscopy and bold line represent AuNPs alone with absorption wavelength at 530 nm, dotted line represent AuNPs + BSA with high intensity (arbitrary units) and wavelength at 539 nm compared to bold dotted line which represent AuNPs + Hhsp70 with reduced intensity and absorption peak at 539 nm. Absorbance (a.u) represents arbitrary units and wavelength (nm) represents distance between adjacent peaks in nanometer.

AuNPs present further red-shift in absorption wavelength with a peak at 539 nm when they interact with BSA compared to 538 nm absorption wavelength peak of AuNPs interaction with Hhsp70 (Fig 3.5B). Since AuNPs were capped with cysteine, the disulfide bonds and electrostatic bonds exist between the cysteine capped AuNPs and the respective protein may facilitate the interaction. TEM images further confirmed that AuNPs pre-incubated with BSA exhibited a protein 'corona' around them (Fig 3.6). BSA modified both the size and the shape of visualised AuNPs complex as previously reported by Horovitz *et al* (2007) (Fig 3.6). Thus, AuNPs are capable of interacting with BSA as confirmed by the UV/vis spectroscopy analysis (Fig 3.5B).

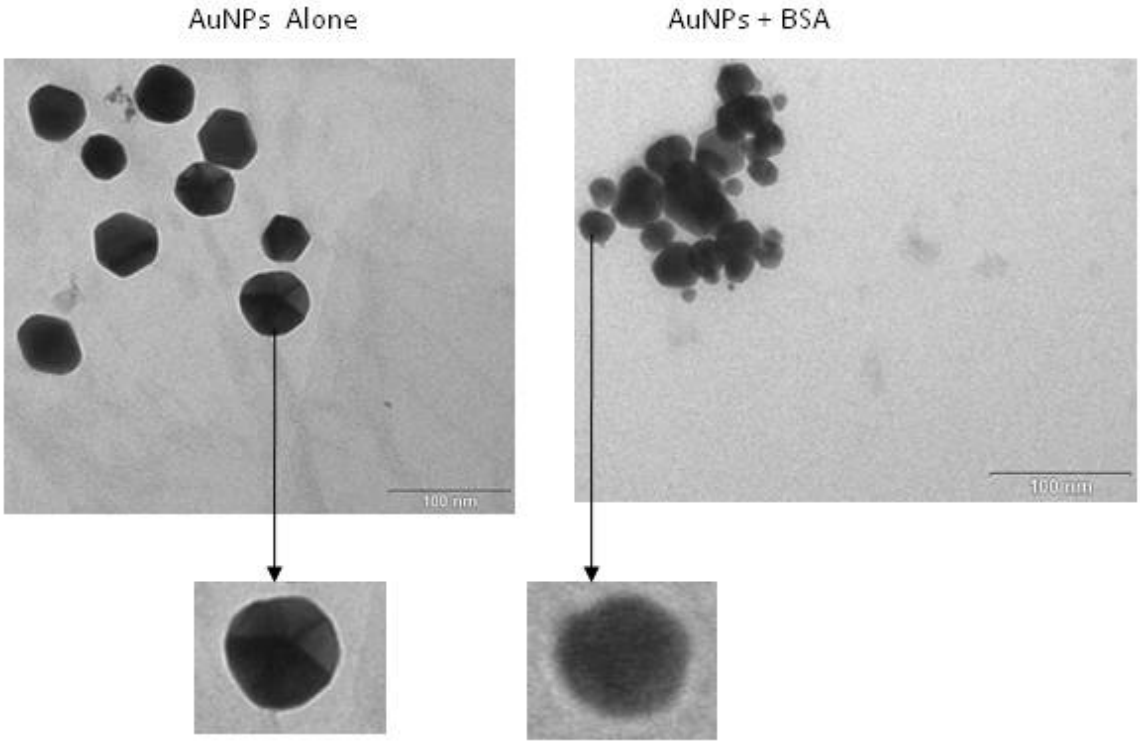

Figure 3.6 TEM micrographs of AuNPs with BSA
Transmission electron microscopic images of the interaction between AuNPs and BSA, (A) image representing AuNPs alone and pulled down image represent a single spherical shaped AuNP (B) image signifying agglomerated AuNPs caused by coating AuNPs with BSA which give raise to the protein-protein interaction and pulled down image represent a single AuNP with protein coat on its surface.

3.2.1 Interaction of AuNPs and BSA in a pH dependant fashion

This study was conducted to observe the effect of varying pH conditions on the interaction of AuNPs with BSA. The reaction was conducted at 1.6, 4.6, 8.0 and 10.5 pH values (Fig 3.7). To confirm the formation of aggregates between AuNPs and BSA, UV/vis spectra of products were assessed. First it was important to establish the UV/vis spectra of AuNPs alone so that any modification on the UV/vis absorption wavelength would be due to interaction of proteins with AuNPs.

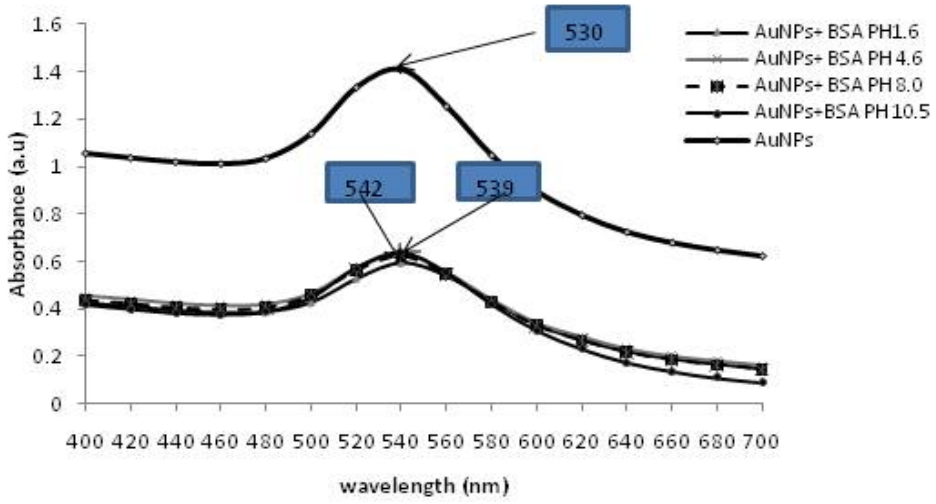

Figure 3.7 Effect of pH in the interactions of AuNPs with BSA
pH influence on the interaction of 1.086 x 10^{-5} mol/l AuNPs with 0.01mg/ml BSA, bold solid line represent AuNPs alone with high intensity and absorption wavelength peak at 530 nm, BSA with pH ranges at 4.6; 8.0 and 10.5 showed wavelength peaks at 539 nm, BSA with pH values at 1.6 absorbed at longer wavelength with peak at 542 nm. Absorbance (a.u) represents arbitrary units and wavelength (nm) represents distance between adjacent peaks in nanometer.

The UV/vis spectroscopic profile of AuNPs was characterised by an absorption wavelength peak at 530 nm. The presence of BSA pH 4.6, 8.0 and 10.5 respectively, red-shifted the absorption peak to 539 nm. The presence of BSA with pH value 1.6 further red-shifted the absorption wavelength to 542 nm (Fig 3.7). This suggests that the interaction of AuNPs and BSA is influenced by varying pH conditions *in vitro*.

3.2.2 Interaction of AuNPs and BSA in a concentration dependant fashion

To show that the interaction of AuNPs with BSA is specific at neutral pH, the reaction was repeated at various concentrations of BSA (0.02 mg/ml, 0.05 mg/ml and 0.1 mg/ml) and 1.086 x 10^{-5} mol/l AuNPs (Fig 3.8). The addition of varying concentrations of BSA to AuNPs was expected to result in unique AuNPs + BSA complexes of characteristic spectroscopic features (Horovitz *et al*., 2007). However, it was observed that increased protein concentrations had no significant effect on the interaction of BSA with AuNPs (Fig 3.8). It is possible that AuNPs were fully saturated on their surfaces at the lowest concentration of BSA used in this study.

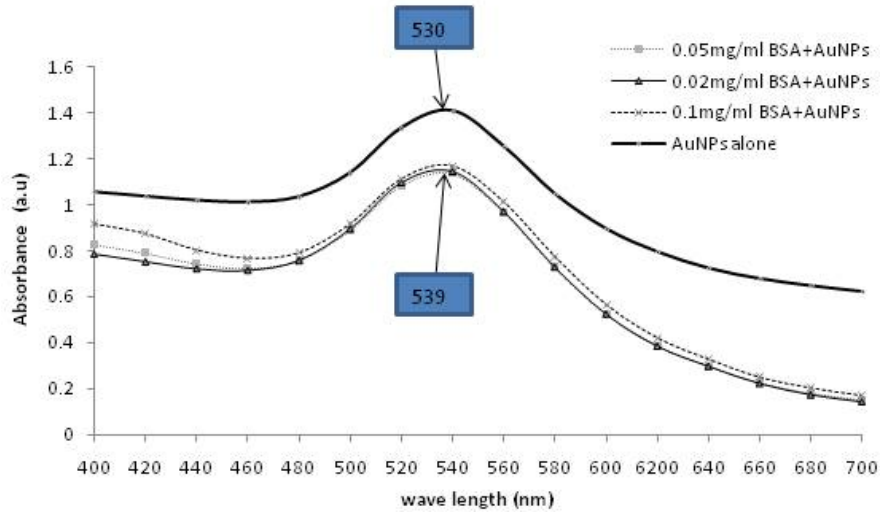

Figure 3.8 Effect of varying BSA concentration in the interaction of AuNPs with BSA
Evaluation of AuNPs interaction with BSA as concentration dependent, bold line implies to1.086 x 10^{-5} mol/l AuNPs alone with absorption wavelength at 530 nm, bold dotted line represent 1.086 x 10^{-5} mol/l AuNPs + 0.1mg/ml of BSA, dotted line represent 1.086 x 10^{-5} mol/l AuNPs + 0.05mg/ml of BSA, solid line represent 1.086 x 10^{-5} mol/l AuNPs + 0.02mg/ml of BSA.

3.3 AuNPs suppressed heat induced aggregation of MDH and CS

MDH and CS are known to aggregate when subjected to heat stress, and Hsp70 has been demonstrated to suppress the aggregation of MDH *in vitro* (Shonhai *et al*., 2008). The C- terminal substrate binding domain of Hsp70 is responsible for its interaction with

peptide (Demand *et al*., 1998). Similarly, small heat shock proteins have been associated to interact with CS (Ahrman *et al*., 2007).

This study sought to investigate the effect of AuNPs on the stability of MDH under heat stress *in vitro*. First, the aggregation of MDH (alone) in response to heat stress was confirmed (Fig 3.9). Upon heating MDH (alone) for 30 mins, the protein aggregated as was observed by turbidity measurement at 360 nm. It is known that Hsp70 proteins are capable of suppressing heat induced aggregation of MDH (Shonhai *et al*., 2008). To confirm this, MDH was heated at 48^{o}C in the presence of Hhsp70 and it was observed that the aggregation of MDH was suppressed.

Similarly, it was curious to investigate the effect of AuNPs on the stability of MDH against heat stress. AuNPs (0.065 x 10^{-5} mol/l) were added to 0.65 µM MDH and the reaction was allowed to proceed at 48^{o}C (Fig 3.9). It was observed that AuNPs were capable of suppressing MDH aggregation. Next, AuNPs (0.065 x 10^{-5} mol/l) were added to a mixture of 0.65 µM MDH + 1.3 µM Hhsp70 and it was found that, AuNPs promoted further the activity of Hhsp70 with respect to its suppression of heat-induced aggregation of MDH (Fig 3.9). As a control, it was determined if AuNPs alone may contribute to increase in turbidity at 48^{o}C. No increase in turbidity was observed when AuNPs were heated at 48^{o}C. This confirms that, AuNPs were not only stable, but were also able to protect MDH from heat-induced aggregation.

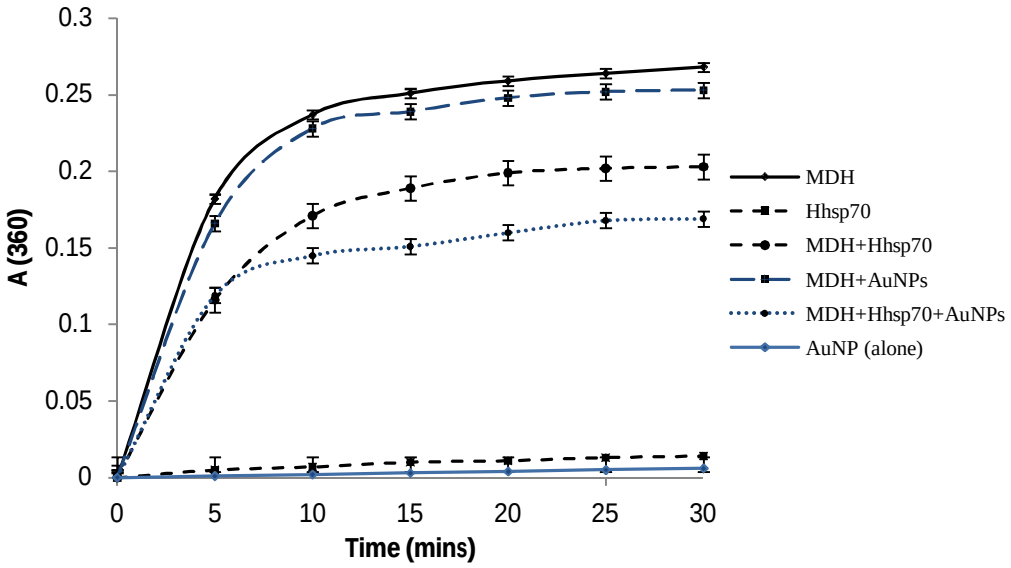

Figure 3.9 Capability of AuNPs to suppress protein aggregation under heat-induced stress condition

The aggregation of 0.65 µM MDH alone, in the presence of 1.3 µM Hhsp70 and in the presence of 0.065 x 10^{-5}mol/l AuNPs was monitored spectrophotometrically at 360 nm, at 48^{o}C for 30 mins. This experiment was repeated using complex of MDH + Hhsp70 with 0.065 x 10^{-5} mol/l AuNPs.

Ahrman *et al* (2007) demonstrated the suppression of citrate synthase aggregation by sHsp. This study sought to investigate the effect of AuNPs on the stability of CS against heat stress *in vitro*. First, the aggregation of CS alone in response to heat induced stress was confirmed (Fig 3.10). Upon heating CS alone for 45 mins, as expected the protein aggregated as was observed by turbidity measurement at 360 nm. It was inquisitive to assess the effect of AuNPs on the aggregation of CS at 48^{o}C. AuNPs (0.065 x 10^{-5} mol/l) were added to 0.65 µM CS and the reaction was allowed to proceed at 48^{o}C. It was observed that AuNPs were capable of suppressing CS aggregation. The reaction was repeated using various AuNPs concentrations (0.13 x 10^{-5}, 0.19 x 10^{-5}, 0.26 x 10^{-5} and 0.54 x 10^{-5} mol/l) in the presence of 0.65 µM CS. It was observed that AuNPs are capable of suppressing CS aggregation induced by heat stress in a concentration dependent fashion (Fig 3.10).

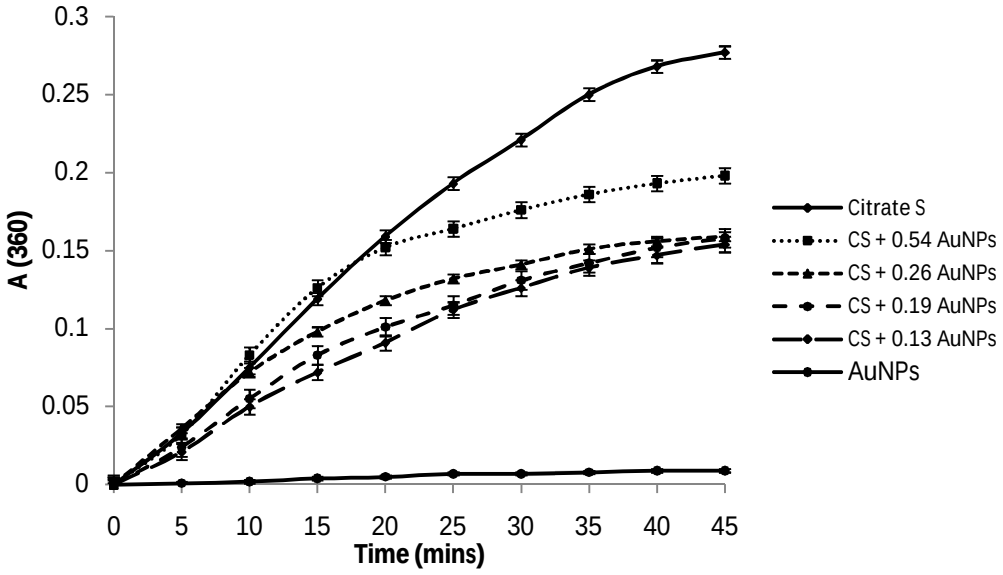

Figure 3.10 Effects of varied AuNPs concentrations on citrate synthase aggregation
Aggregation of 0.65 µM CS, small dots represent CS in the presence of 0.54 x 10^{-5} mol/l AuNPs, followed by CS in the presence of 0.26 x 10^{-5}mol/l of AuNPs, followed by CS in the presence of 0.19 x 10^{-5}mol/l of AuNPs and lastly dashed line represent CS in the presence of 0.13 x 10^{-5}mol/l of AuNPs were monitored in the spectrophotometer at 360 nm at 48^{o}C for 45 mins.

3.3.1 AuNPs were capable of suppressing heat-induced aggregation of MDH in a concentration dependant fashion

The study sought to investigate the effect of varying AuNPs concentrations on the stability of MDH during heat stress *in vitro*. Following previously observed effects of AuNPs on the stability of MDH (Fig 3.9). The concentration of AuNPs was varied (0.13 x 10^{-5}, 0.54 x 10^{-5}, 0.64 x 10^{-5} and 0.86 x 10^{-5} mol/l) and their effect on the stability of MDH was measured by measuring turbidity changes at 360 nm at 48^{o}C for 30 mins. It was observed that AuNPs were capable of suppressing MDH aggregation in a concentration dependant fashion (Fig 3.11). This confirms that AuNPs inhibited MDH aggregation, in a specific way.

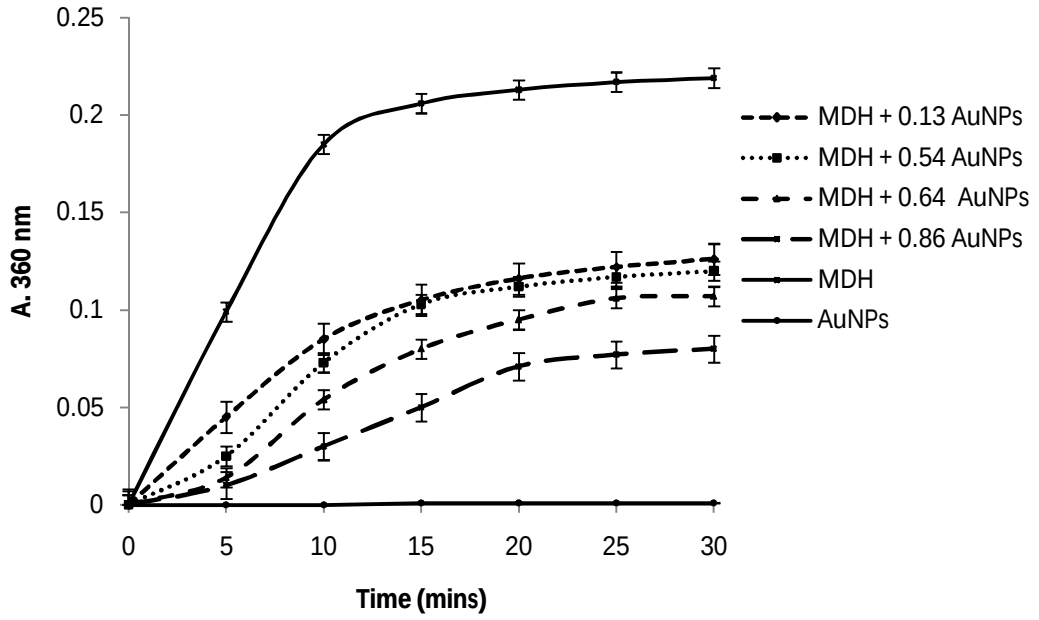

Figure 3.11 Effect of different AuNPs concentrations in the aggregation of MDH under heat induced stress

Aggregation of 0.65 µM MDH alone (MDH), MDH in the presence of 0.13 x10^{-5}mol/l AuNPs, MDH in the presence of AuNPs 0.54 x 10^{-5}mol/l, MDH in the presence of AuNPs 0.64 x 10^{-5}mol/l, MDH in the presence of AuNPs 0.86 x 10^{-5}mol/l was monitored spectrophotometrically at 48^{o}C at 360 nm for 30 mins.

3.4 AuNPs maintained CS and MDH in soluble forms in the presence of heat stress

Since it was observed that AuNPs could suppress heat-induced aggregation of MDH and CS *in vitro*, it was important to investigate the solubility status of the two proteins in the presence and absence of AuNPs. Briefly, 1 µM MDH and 1 µM CS were heated at 48^{o}C in the presence and absence of 0.108 x 10^{-6} mol/l AuNPs. The products were centrifuged at 14,000 g to separate soluble and insoluble fractions and mixed with SDS loading buffer and boiled at 95 -100^{o}C before they were analysed with SDS-PAGE. In the absence of AuNPs, MDH and CS appeared aggregated (lane P2 and lane P4), and in the presence of AuNPs, MDH and CS appeared in the pellet and supernatant more or

less equally (lane P1;S1 and lane P3;S3) suggesting that AuNPs were capable of suppressing CS and MDH aggregation against heat stress (Fig 3.12).

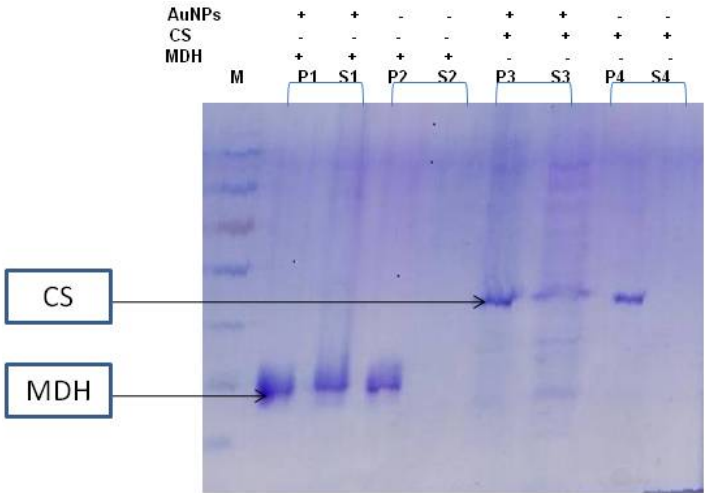

Figure 3.12 AuNPs maintained MDH and CS in soluble forms under heat stress
Evaluation of the capability of AuNPs to suppress aggregation of malate dehydrogenase and citrate synthase invitro, 1 µM CS and 1 µM MDH were incubated at 48^{o}C for 20 mins in the presence and absence of AuNPs (0.108 x 10^{-6} mol/l). After centrifugation soluble fraction (supernatant S) was separated from aggregated fraction (pellet P) and examined by SDS-PAGE.

Chapter 4

Discussion

AuNPs synthesised through concentrations of $AuCl_3$, $NaBH_4$, cysteine and varied reaction times considered to be not optimum had absorption features that were uncharacteristic of AuNPs (Fig 3.2). Results observed showed strong blue shifts in absorption wavelengths peaks around 365 - 375 nm (Fig 3.2). However, Sarangi et al (2007) reported that, these wavelength peaks suggest for the presence of monodispersed spherical shaped AuNPs (Müller *et al*., 2002; Gao *et al*., 2005). AuNPs synthesised using optimised concentrations of $AuCl_3$, $NaBH_4$, cysteine and varied reaction time (see methods, section 2.1.1) had absorption features that were characteristic of AuNPs (Fig 3.3).

AuNPs synthesised following optimised Turkevich protocol presented an absorption wavelength peak around 530 nm which is attributed to the plasmon resonance mode of spherical gold nanoparticles (Fig.3.3) The surface plasmon resonance (SPR) peak depends on the dielectric properties and the size and shape of the products (Sarangi *et al*., 2007). It is also influenced by the preparation medium and resonance energy. In turn, the resonance energy modifies the refractive index of the preparation medium due to the interaction between oscillating electrons and the positive charged nanoparticle (Müller *et al*., 2002). Chemical interaction between the nanoparticle and the environment also influence the absorption wavelength spectrum (Malvaney, 1996).

Cysteine capped AuNPs synthesised at three various time intervals using 0.1 M $AuCl_3$, 1 M $NaBH_4$ and 33 mM cysteine exhibited SPR mode for spherical AuNPs (Chen *et al*., 2005), owing to their absorption wavelength peaks and their red-wine colour. AuNPs synthesized for 2 hours presented high intensity and absorption peaks at 535 nm compared to intermediate intensity of AuNPs synthesized for 30 mins with absorption peaks at 530 nm and reduced intensity with red shifted absorption peaks at 540 nm of AuNPs synthesised for 5 mins (Fig 3.3). Products obtained in the study displayed features resembling those previously obtained by Chili *et al* (2008).

The observed wavelength peaks of obtained AuNPs suggest the presence of a mixture of AuNPs dominated by spherical shapes. This is thought to be due to isotropic oscillations which are the same in all directions, as explained by the principle of SPR (Chen *et al*., 2005). The UV/vis absorption spectra peaks of AuNPs were not significantly changed for at least one month of preparations signifying AuNPs stability.

TEM micrographs of AuNPs obtained in this study presented AuNPs with varying shapes; spherical shaped AuNPs dominated in samples synthesised for 30 mins and 5 mins (Fig 3.4). AuNPs exhibiting hexagonal shape were dominant in samples synthesised for 2 hours (Fig 3.4). To obtain the desired size and shape (spherical shape with diameter below 50 nm), $AuCl_3$, $NaBH_4$ and cysteine were used at these concentrations: 0.1 M $AuCl_3$, 1 M $NaBH_4$, 33 mM cysteine, respectively. TEM micrographs of batches prepared for 5 and 30 minutes presented particles that were predominantly spherical in shape with diameters ranging from 35 nm - 55 nm (Fig 3.4).

The batch prepared for 2 hours was dominated by a mixture of hexagonal, pentagonal and spherical shaped AuNPs with diameters ranging from 25 nm - 45 nm (Fig 3.4). It was observed from these experiments that, the nanoparticle size and morphology depend on experimental parameters such as the core material, the reducing agent and the capping agent.

The formation of AuNPs is influenced by interplay of events such as the nucleation, growth and coagulation of the reactants (Turkevich, 1985). Yang *et al* (2007) presented the formation of mixed shaped AuNPs in the presence of citric acid and PVP as capping agent. Horovitz *et al* (2007) presented the formation of 48 ± 5 AuNPs that were predominantly spherical in shape using citrate reduction method.

The interaction of 1.086 x 10^{-5} Mol/l AuNPs with 0.01 mg/ml of Hhsp70 and BSA respectively *in vitro* were analyzed using UV/vis spectroscopy (Fig 3.5B). AuNPs complexed with BSA and with Hhsp70 presented red-shifted absorption wavelengths peaks at 539 and 538 nm, respectively. The shift in absorption wavelengths and the drop in intensity of arbitrary units suggest that there were specific interactions between AuNPs and proteins (BSA, Hhsp70).

AuNPs appeared to interact with BSA preferentially compared to Hhsp70 (Fig 3.5B). This is shown by the UV/vis spectra analysis (Fig 3.5B). It is thought that the cysteine positioned at the residue number 34 in albumin possesses SH groups that are prone to form mixed disulphide bonds with other proteins (Alexis *et al*., 2008). It may be argued

that the SH groups in the cysteine coating AuNPs is positioned to interact with BSA better than Hhsp70. However this remains to be further validated.

The binding constants between AuNPs and specific proteins are not yet fully understood. In future it is important to establish this for various combinations of AuNPs and specific proteins as it may be useful in predicting the specific proteins that may interact with AuNPs in a given proteins mixture. The binding constants (*k*) for serum proteins and AuNPs were previously found to range between (10^4 - 10^7 mol/l) (Linse *et al*., 2007). This range had been reported for amino acids coated AuNPs interacting with chymotrypsin (Lundgvist *et al*., 2004). The binding constant has been reported to increase with the increase of AuNPs diameter (Silvia *et al*., 2010). Jiang *et al* (2006) observed similar binding constant on herceptin coated AuNPs interaction with $ErbB_2$.

It is possible to confirm the interaction between AuNPs and proteins using transmission electron microscope (Horovitz *et al*., 2007). In the study, TEM micrographs of AuNPs + BSA presented AuNPs with a ‘coat’ or a corona on their surfaces as evidenced by the disappearance of distinct crystal-lines that are visible in AuNPs viewed in the absence of BSA compared to those pre-mixed with BSA (Fig 3.6). The ‘BSA-coated’ AuNPs appeared slightly enlarged (Fig 3.6), compared to those that were not exposed to the protein.

The formation of mixed disulfide bonds between AuNPs and BSA ‘coat’ resulted in the accumulation of protein surface on AuNPs thus invoking interaction between cysteine

coated AuNPs and proteins, leading to AuNPs agglomeration. The sample of AuNPs + BSA was red-wine in colour and the absorption wavelength peak was not significantly changed for at least 2 weeks of its preparation as analyzed by the UV/vis spectroscopy. The red shift observed when proteins interact with AuNPs may be due to the change in the dielectric constant as a result of an increase in diameter of the protein coated AuNPs.

Nanoparticles are known to travel in biological fluids as proteins coated entities (Lynch *et al*., 2007). Effectively, the nanoparticle unit in cell is believed to be the nanoparticle and its corona and not the original nanoparticle as such (Lynch *et al*., 2006; Cedervall *et al*., 2007). Thus nanoparticle protein interaction is an important process as the behavior of the nanoparticles and its fate may indeed depend on the proteins that characterise its surface.

UV/vis spectroscopy was further used to observe the effect of experimental parameters such as varying pH on the interaction of AuNPs with BSA. The reaction was conducted for BSA at pH values of 1.6, 4.6, 8.0 and 10.5. The variation in pH conditions had influence on the interaction between AuNPs and BSA (Fig 3.7). At pH 1.6, the AuNPs+BSA complex exhibited a red-shift in absorption spectral distinct from that of AuNPs alone (Fig 3.7). The low pH (1.6) may have resulted in the change of the protein's overall net charge, thus promoting interaction between AuNPs and BSA better. Surface charge is known to be one of the factors that influence most biomolecular interactions and it is thought that the same phenomena apply in the interaction of

AuNPs with BSA (Li-Mei *et al*., 2006). Indeed, extreme pH variation may influence the interaction of proteins with AuNPs as observed in this study and confirmed previously (Foster, 1977; Li-Mei *et al*., 2006).

It was important to assess if the interaction of AuNPs and BSA at the above mentioned pH points is specific, therefore, reactions were repeated at different BSA concentrations (Fig 3.8). The interaction of BSA with AuNPs was concentration independent at pH 7.4 (Horovitz *et al*., 2007). This suggests that the change in absorption spectra in AuNPs+BSA mixture was due to specific AuNPs+BSA interaction rather than a mere shielding of AuNPs by BSA. However, the variation in BSA concentration only resulted in modest change in absorption peaks. This may be because AuNPs were fully saturated by the protein at the lowest concentration of protein used.

MDH is known to aggregate at 48^{o}C (Shonhai *et al*., 2008). In the presence of chaperones, MDH aggregation is suppressed at 48^{o}C (Shonhai *et al*., 2008). This model was adopted to investigate the effect of AuNPs on MDH aggregation at 48^{o}C. MDH (in the absence of BSA and Hhsp70) aggregated at 48^{o}C as expected (Fig 3.9) (Shonhai *et al*., 2008). Upon repeating the assay in the presence of Hhsp70, the latter was capable of suppressing heat-induced aggregation of MDH marginally (Fig 3.9). AuNPs were first subjected to heat stress at 48^{o}C and their aggregation was evaluated spectroscopically. AuNPs alone did not aggregate at 48^{o}C (Fig 3.9). This may be due to their melting and boiling points being above 48^{o}C. Their effects on MDH aggregation was evaluated by monitoring turbidity of MDH at 48^{o}C in the presence of AuNPs at increasing

concentrations (Fig 3.11). It was observed that the increase in AuNPs concentrations resulted in enhanced suppression of MDH aggregation (Fig 3.11). It was also further observed that in the presence of AuNPs, Hhsp70 suppressed aggregation of MDH better (Fig 3.9). This confirms that AuNPs may possess chaperone activity.

It was further evaluated if AuNPs had influence on the solubility of proteins subjected to heat stress at 48^{o}C. MDH and CS were subjected to heat stress at 48^{o}C in the presence and in the absence of AuNPs. The solubility status of the two proteins were subsequently evaluated (Fig 3.12). In the absence of AuNPs, MDH and CS precipitated as insoluble products (Fig 3.12, lane P2 and lane P4), however in the presence of AuNPs, nearly 50% of both MDH and CS were maintained in soluble forms at 48^{o}C, samples pre-incubated for 20 mins (Fig 3.12, lane P1;S1 and lane P3;S3). This further confirms that, AuNPs have chaperone function and that they are capable of maintaining proteins in soluble form during heat stress. The fact that AuNPs are capable of protecting proteins from heat induced stress is interesting. Firstly, AuNPs may be seen as unlikely to be toxic, since their interaction with proteins may not induce negative conformational changes to the latter. In addition, the stabilising effect of AuNPs on proteins makes AuNPs amenable for bio-conjugation in AuNPs-protein complexes used in bio-imaging and diagnostics. In this case, the AuNPs may play not only an imaging role, but may also stabilize proteins (enzymes). This is especially important in the design of field kits.

Chapter 5

Conclusion and Future work

Gold nanoparticles were successfully synthesised using a slightly modified citrate reduction method at room temperature (Turkevich *et al*., 1951). Observations from gold nanoparticles synthesis suggested that varying parameters such as the reducing agent, capping agent, gold salt and reaction time had significant influence on the size and the morphology of prepared gold nanoparticles.

The interaction of gold nanoparticles with Hhsp70, BSA, MDH and CS was established. BSA seemed to interact with AuNPs better than Hhsp70. The fact that AuNPs may interact with proteins to stabilize their functional status holds promise in both drug design and immuno-diagnostics.

In future, it will be important to investigate the interaction kinetic between serum proteins and AuNPs and to understand the functional perturbation of proteins induced by AuNPs interaction. In addition, it would be important to investigate the biomolecular mechanism in which AuNPs inhibit aggregation of MDH and CS. These findings may potentially divulge important information that may possibly lead to the use of AuNPs to prevent aggregation of heat sensitive enzyme for both commercial and research purposes.

Bibliography

Ahrman, E., Wietske, L., Andrew, A.J., Carol, R.V., Cecilia, S.E. Chemical cross-linking of the chloroplast localized small heat-shock protein, Hsp21, and the model substrate citrate synthase. *Protein Science*. (2007). **16**:1464–1478.

Alper, C.A. Plasma Protein Measurements as a Diagnostic Aid. *N Eng J Med.* (1974). **291**:287-290.

Andrievskii, R. A. Directions in Current Nanoparticle Research. *Powder Metallurgy and Metal Ceramics*. (2003). **42**: 624-629.

Astruc, D., Daniel, E.T. Nanotechnological applications of materials. *J.Phys. Chem. B.* (2003). **11**: 431-439.

Banker, M.J., Clark, T.H., Williams, J.A. Development and validation of a 96-well equilibrium dialysis apparatus for measuring plasma protein binding, *J. Pharm*. *Sci.* (2003). **92**:967–974.

Basha, E., Lee, G., Demeler, J. B., Vierling, E.E. Chaperone activity of cytosolic small heat shock proteins from wheat. *Eur. J. Biochem*. (2004). **271**: 1426-1436.

Bertucci, C., Domenici, E. Reversible and Covalent Binding of Drugs to Human Serum Albumin: Methodological Approaches and Physiological Relevance. *Curr. Med. Chem.* (2002). **9**:1463–1481.

Bianco, A., Kostarclos, K., Partidos, C.D., Prato, M. Biomedical application of functionalized carbon nanotubes. *Chem..commun*. (2005). **5**:571-577.

Blunk, T., Hochstrasser, D.F., Sanchez, J.C., Muller, B.W., Muller, R.H. Colloidal carriers for intravenous drug targeting: plasma protein adsorption patterns on surface modified latex particles evaluated by two-dimensional polyacrylamide gel electrophoresis. *Electrophoresis.* (1993). **14**:1382–1387.

Bredig, G. development of an arc method for colloidal gold nanoparticles *ang.chem*.(1898). **11**:952.

Bruchez, M., Moronne, M., Gin, P., Weiss, S., Alivisatos, A.P. Semiconductor nanocrystals as flurescence biological labels. *Science.* (1998). **281**: 2013-2016.

Cassagneau, T., Fendler, J.H. Preparation and layer by layer self assembly of silver nanoparticles capped by graphite oxide nanosheets. *J.Phys. Chem. B.* (1999). **103**: 1789-1793.

Cedervall, T., Lynch I., Foy, M., Berggard, T., Donnelly, S.C., Cagney, G. Detailed identification of plasma proteins adsorbed on copolymer nanoparticles. *Angew Chem Int Ed Engl*. (2007). **46**:5754-5756.

Cedervall, T., Lynch, I., Stina, L., Berggard, T., Thulin, E., Nilsson, H., Kenneth, A.D., Linse, S. Understanding the nanoparticle–protein corona using methods to quantify exchange rates and affinities of proteins for nanoparticles. *Chem Int Ed Eng*.(2006).**13**:110-116.

Cedervall, T., Lynch, I., Foy, M., Berggard, T., Donnelly, S.C., Cagney, G., Linse S., Dawson, K.A. Detailed identification of plasma proteins adsorbed on copolymer nanoparticles, Angew. *Chem., Int. Ed. Engl*. (2007). **46**:5754–5756.

Cedervall, T., Lynch, I., Lindman, S., Berggard, T., Thulin, E., Nilsson, H., Dawson, K.A., Linse, S. Understanding the nanoparticle–protein corona using methods to quantify exchange rates and affinities of proteins for nanoparticles, *Proc. Natl. Acad. Sci. U. S. A*. (2007). **104**:2050–2055.

Chen, Y., Gu, X., Nie, C.G., Jiang, Z.Y., Xie, Z.X., Lin, C.J. Gold nanoparticles synthesis: UV/vis spectroscopy analysis. Chem Commun (2005), **5**: 4181–4193.

Check, E. Gene therapy: a tragic setback. *Nature.* (2002). **420**:116–118.

Chili, M.M., Revaprasadu, N., Synthesis of anisotropic gold nanoparticles in a water soluble polymer. *Materials Letters*. (2008). 3896-3899.

Chiao, D.J., Shyu, R.H., Hu, C.S., Chiang, H.Y., Tang, S.S. *J. Chromatogr B.* (2004). **37:**809.

Chithrani, B.D., Ghazani, A.A., Chan, W.C. Determining the size and shape dependence of gold nanoparticle uptake into mammalian cells, *Nano Lett*. (2006). **6**:662–668.

Daniel, M.C., Astruct, D., *editors. Chem. Rev*. (2004).**104**: 293-346.

Demand, J., Luders, J., Hőhfeld, J. The carboxy-terminal of Hsc 70 provides sites for a distinct set of chaperone cofactors. *Mol. Cell. Biol*. (1998). **18**: 2023-2028.

Deyl, Z. Electrophoresis: A survey of techniques and applications. *Elsevier Scientific*. (1983), **83**: 90170-90177.

Dobrovolskaia, M.A., McNeil, S.E. Immunological properties of engineered nanomaterials. *Nat. Nanotechnol.* (2007). **2**: 469-478.

Dobson, J. Magnetic nanoparticles for drug delivery. *Drug.Del.Res*. (2006). **67**:55-60.

Dutta, D., Sundaram, S. K., Teeguarden, J.G., Riley, B. J., Fifield, L.S., Jacobs, J.M., Addleman, S.R., Kaysen, G.A., Moudgil, B.M., Weber, T.J. Adsorbed proteins influence the biological activity and molecular targeting of nanomaterials. *Toxicology Sci*. (2007).**100**: 303–315.

Elliot, W.H., Elliot, C.D. Biochemistry and molecular biology. *Oxford University express.* (2005).**3**:108-117.

Ellis, J. Proteins as molecular chaperones. *Nature*. (1987). **328**: 378-79.

Faraday, M. Preparation and properties of colloidal gold nanoparticles *phil.Trans* (1957).147,145.

Fei, Q., Xiao, D., Zhang, Z., Huan, Y., Feng, G. A novel silica-coated multiwall caron nanotubes with CdTe quantum dots nanocomposite molecular and biomolecular spectroscopy. *Surface and interface materials*. (2009), 597-601.

Feldmann, Appl. Phys. Lett. (2002). **81**:171.

Fischer, H.C., Chan, W.C., Nanotoxicity: The growing need for *in vivo* study. *Curr.pin. Biotechnol.* (2007) **18**: 565-571.

Foster, J.F., Albumin Structure, Function, and Uses*. Oxford:Pergamon Press.* (1977). 53–84.

Franker, S.P., Medical uses of gold compounds, *Gold bulletin*, (1996). 29-32.

Frank, J.M., Joseph G. M., Is Bovine Albumin to Complex to be just a commodity? *Bioprocess technical*. (2010).

Gao, D.Y., Tian, S., Bi, Y., Chen, A., Yu, G., Zhang, H. Part A, *Spectrochim. Acta*, (2005) **62**,:1203.

Gao, Y., Bi, Y., Chen, A. Interchain Disulfide Bonds Promote Protein Cross-Linking During Protein Folding. *J. Biochem.*, (2001).**129**:179–183.

Gobin, A. M., Lee, M. H., Halas, N. J., James, W. D., Drezek, R. A., West, J. L. Near-Infrared Resonant Nanoshells for Combined Optical Imaging and photothermal Cancer Therapy. *Nano Lett.* (2007),***7***:1929–1934.

Goppert, T.M., Muller, R.H. Adsorption kinetics of plasma proteins on solid lipid nanoparticles for drug targeting, *Int. J. Pharm*. (2005) **302**:172–186.

Goppert, T.M., Muller, R.H. Protein adsorption patterns on poloxamer- and poloxamine-stabilized solid lipid nanoparticles (SLN), *Eur. J. Pharm. Biopharm*. (2005). **60**:361–372.

Gosh, P., Man, G., De, M., Chae, K.K., Rotello, V.M. Gold nanoparticles in delivery application. *Advanced delivery reviews*. (2008). **60**:1307-1315.

Gutwein, L.G., Webster, T.J. Affects of alumina and titania nanoparticulates on bone cell function. *American Ceramic Society 26 th Annual Meeting Conference Proceedings* (2003).

Harnisch, S., Muller, R.H. Adsorption kinetics of plasma proteins on oil-in-water emulsions for parenteral nutrition, *Eur. J. Pharm. Biopharm*. (2000). **49**:41–46.

Heegaard, P.M., Boas, U., Otzen, D.E. Dendrimer effects on peptide and protein fibrillation. *Macromol. Biosci.* (2007).**7**: 1047-1059.

Hoffman, T.J., Sieckman, G.L., Volkert, W.A., Truman, H.S. Iodinated bombesin analogues: Effect of N-terminal vs side chain iodine attachment on BBN/GRP receptor binding. *Journal of Nuclear Medicine.* (1999).**37**: 850-855.

Holmes, P. Airborne Particles: Exposure in the Home and Health Effects; Leicester, *MRC Instit. Environ*. Health (2000).

Horovitz, O., Gheorghe, T., Aurora, M., Traianos, Y., Maria, T.C. Protein binding to gold nanoparticles. *Gold bulletin*. (2007). 4013.

Huang, J., Li, Q., Sun, D., Lu, Y., Su, Y., Yang, X., Wang, H., Wang, Y., Shao, W., He, N., Hong, J., Chen, C. Biosynthesis of silver and gold nanoparticles by novel sun dried leaf *Cinnamomum camphora*. *nanotechnology journal*. (2007). **18**:104-105.

Huang, T., Murray, R.W. Quenching of [Ru(bpy)3]2+ fluorescence by binding to Au nanoparticles. *Langmuir*, (2002). **18**:7077–7081.

Huang, H.L., Xu, Y.G., Low, H.Y. Effects of Film Thickness on Moisture Sorption, Glass Transition Temperature and Morphology of Poly(chloro-*p*-xylylene) Film. *Polymer,* (2005) **46**: 5949–5955.

Ito, A., Shinkai, M., Honda, H., Kobayashi, T. Medical application of functionalized magnetic nanoparticles. *J. Biosci.Bioeng*. (2005). **100** (1):1-11.

Jain, P.K., Lee, K.S, El-Sayed I.H., Calculated absorption and scattering properties of gold nanoparticles of different size, shape, and composition: applications in biological imaging and biomedicine. *J Phys Chem B*. (2006).**110**:7238-7248.

Jain, P.K., El-Sayed I.H. Biomedical applications of gold nanoparticles of different size, shape, and composition. *J Phys Chem B*. (2007).**72**:32-39.

Jennings, T.L., Singh, M.P., Strouse, G.F. Fluorescent Lifetime Quenching Near *d*1.5 nm Gold Nanoparticles: Probing NSET Validity. *J. Am. Chem. Soc.* (2006). **128**: 5462–5467.

Jong, D.e., Borm, W.H., P.J. Drug delivery and nanoparticles: applications and hazards. *Int. J. Nanomedicine* ,(2008). **3**: 133-149.

Josephson, L. Magnetic nanoparticles for MR Imaging. *BioMEMS.Biomed. Nanotechnol*. (2006)**1**: 227-237.

Kamat, P.V., Shanghavi B. Interparticle Electron Transfer in Metal/ Semiconductor Composites:Picosecond Dynamics of CdSCapped Gold Nanoclusters. *J. Phys. Chem. B* (1997).**101**: 7675- 7679.

Kamat, P.V., Flumiami, M., Hartland, G.V. *J. Phys. Chem. B.* (1999). **102**:3123.

Kim, H.R., Andrieux, K., Delomenie, C., Chacun, H., Appel, M., Desmaele, D., Taran, F., Georgin, D., Couvreur, P., Taverna, M. Analysis of plasma protein adsorption onto PEGylated nanoparticles by complementary methods: 2-DE, CE and Protein Labon- chip system, Electrophoresis. (2007). **28:**2252–2261.

Kreibig, U., Volmer, M. *Optical Properties of Metal Clusters*; Heidelberg:Springer-Verlag.(1995).

Laemmli, U. K. Cleavage of structural proteins during the assembly of the head of bacteriophage T4. *Nature,* (1970), **227**: 680-685.

Liberek, K., Marszalek, J., Ang, D. Georgopoulos, C., Zylicz, M. *Escherichia coli* DnaJ and GrpE heat shock proteins jointly stimulate ATPase activity of DnaK. *Proc. Natl. Acad. Sci. U.S.A*. (1991), **88**: 2874–2878.

Liberek, K., Skowyra, D., Zylicz, M., Johnson, C., Georgopoulos, C. The *Escherichia coli* DnaK chaperone, the 70-kDa heat shock protein eukaryotic equivalent, changes conformation upon

ATP hydrolysis, thus triggering its dissociation from a bound target protein. *J.Biol. Chem*. (1991), **266**: 14491-14496.

Li-Mei, A.O., Feng, G.A.O., Bi-feng, P., Da-xiang C., Hong-chen, G. Interaction between gold nanoparticles and bovine serum albumin or sheep antirabbit immunoglobulin G. *chiness journal of chemistry*. (2006). **24**:253-256.

Linse, S., Cabaleiro-Lago, C., Xue, W. F., Lynch, I., Lindman, S., Thulin, E., Radford, S. E., Dawson, K. A. Nucleation of Protein Fibrillation by Nanoparticles. *Proc. Natl. Acad. Sci. U.S.A.* (2007). **104**: 8691–8696.

Link, S., El-Sayed, M.A. Shape and size dependence of radiative, non-radiative and photothermal properties of gold nanocrystals. *Int. ReV. Phys. Chem.* (2000), **19** (3):409-453.

Link, S., Mohamed, M.B., El-Sayed, M.A., *J. Phys. Chem*. B. (1999), **103**:3073.

Liu, X., Atwater, M., Wang, J., Huo, Q. Extinction coefficient of gold nanoparticles with different sizes and different capping ligands, Colloids Surf. B Biointerfaces Dependent bio-catalyzed transformations*. Angew. Chem., Int. Ed*. (2004). **43**:4519–4522.

Liz-Marzan, L. M. Nanometals: Formation and color. *Materials Today (*2004),**7:**26-31.

Loo, C., Lowery, A., Halas, N.J., West, J.L., Drezek, R. Immunotargeted nanoshells for integrated cancer imaging and therapy.*Nano.lett*.(2005),**5**:709-711.

Losin, M., Toderas, F., Baldeck, P.L., Astilean, S. Study of protein-gold nanoparticles conjugation by fluorescence and surface-enhanced Raman scattering.*molstruc*. (2009),**02**:004.

Lu, Y., Sega, E., Leamon, C.P.,Folate receptor-targeted immunotherapy of cancer: mechanism and therapeutic potential. *Adv Drug Deliv Rev*. (2004). **56**:1161–76.

Lundqvist, M., Sethson, I., Jonsson, B. H. Protein Adsorption onto Silica Nanoparticles: Conformational Changes Depend on the Particles' Curvature and the Protein Stability. *Langmuir.* (2004). **20**:10639–10647.

Lynch, I., Dawson, K. A., Linse, S. Detecting cryptic epitopes created by nanoparticles. *Sci. STKE,* (2006),**14**:134–135.

Lynch, I., Cedervall, T., Lundqvist, M., Cabaleiro-Lago, C., Linse, S., Dawson, K.A. The nanoparticle–protein complex as a biological entity; a complex fluids and surface science challenge for the 21st century. *Adv. Colloid Interface Sci*. (2007). 167–174.
Lynch, I. Protein-nanoparticle interaction. *Proc.Natl Acad.Sci.* (2008). 40-47.

Maeda, H., Wu, J., Sawa, T. Tumor vascular permeability and the EPR effect in macromolecular therapeutics: a review. *J Control Release*, (2000). **65**:271–84.

Marina, A., Dobrovolskaia, A.K., Patri, J., Zheng, J., Clogston, D., Nader, A., Parag, A., Barry, W., Neun, B.S., Jennifer, B. H., Scott, E.M. Interaction of colloidal gold nanoparticles with human blood effects on particle size and analysis of plasma protein binding profiles. *Nanomedicine*. (2009) 106-117.

Merkoci, A., Aldevert, M., Marins, S., Alegrets, S. New materials or electrochemical sensing V. nanoparticles for DNA labeling. Trends in analytical chemistry. (2005), **24**:4.

Mie, G. Theory of visualizing gold nanoparticles. *Ann. Phys (Leipzing*). (1909). **25**:377.

Mirkin, C. A., Letsinger, R. L., Mucic, R. C., Storhoff, J. J. A DNA-based method for rationally assembling nanoparticles into macroscopic materials. *Nature.* (1996), **382**: 607–609.

Moghimi, S.M., Hunter, A.C., Murray, J.C. Long-circulating and target-specific nanoparticles: theory to practice. *Pharmacol. Rev*. (2001), **53**:283–318.

Mohamed, M., Volkov, B. V., Link, S., El-Sayed, M. A., *Chem. Phys. Lett*. (2000). **317**:517.

Mornet, S., Vasseur, S., Grasset, F., Duguet, E. Magnetic nanoparticles design for medical diagnosis and therapy. *J.Meter.chem*. (2004).**14**:2161-2175.

Mu, L., Feng, S.S. A novel controlled release formulation for the anticancer drug paclitaxel (Taxol): PLGA nanoparticles containing vitamin E TPGS. *J Control Release*, (2003).**86**:33–48.

Müller, J.C., Sönnichsen, H., Poschinger, G., Plessen, V., Klar, A.T., Feldmann, *J. Appl. Phys. Lett.* (2002),**81**:171.

Mulvaney P, Langmuir ,(1996)**12**,788.

Murdock, R.C., Braydich-Stolle, L., Schrand, A.M., Schlager, J.J., Hussain, S.M. Characterization of nanomaterial dispersion in solution prior to in vitro exposure using dynamic light scattering technique. *Toxicol Sci.* (2008).**101**:239-53.

Murray, C. B., Kagan, C. R., Bawendi, M. G. *Annu. Rev. Mater. Sci. (*2000).**30**:545–610.
Musteata, F.M., Pawliszyn, J., Qian, M.G., Wu, J.T., Miwa, G.T., Determination of drug plasma protein binding by solid phase micro extraction. *J. Pharm. Sci*. (2006). **95**:1712–1722.

Muthusamy, B., *Proteomics* (2005). **5**, 3531.

Nagatani ,N., Tanaka, R., Yuhi, T., Endo, T., Karma, K., Takamura, Y., Taniya, E. Science, Technology on Advance Mater. (2006).106–117.

Nel, A., Xia, T., Madler, L., Li, N. Toxic potential of materials at the nanolevel. *Science.* (2006), **311**:622–627.

Niidome, T., Yamagata, M., Okamoto, Y., Akiyama, Y., Takahishi, H., Kawano, T. PEG-modified gold nanorods with a stealth character for in vivo application. *J control Release.* (2006),**114**:34-37.

Olson, R.E., Christ, D.D. Plasma protein binding of drugs, Annu. *Rep. Med. Chem*. (1996), **31**:327–336.

Owens, D.E., Peppas, N.A. Opsonization, biodistribution, and pharmacokinetics of polymeric nanoparticles, *Int. J. Pharm*. (2006), **307**:93–102.

Ozsoz, M., Erdem, A., Kerman, K., Ozkan, D., Tugrul, B., Topcuoglu, N., Ekren, H., Taylan, M. Strong absorption of colloidal gold nanoparticles, *Eng. Chem*. (2003).**75**:21-81.

Pack, D.W., Hoffman, A.S., Pun, S., Stayton, P.S. Design and development of polymers for gene delivery. *Nat Rev Drug Discov*. (2005).**45**:81–93.

Pan, Y., Neuss, S., Leifert, A., Size-dependent cytotoxicity of gold nanoparticles. *Small*, (2007),**3**:1941–9.

Park, T.G., Jeong, J.H., Kim, S.W. Current status of polymeric gene delivery systems. *Adv Drug Deliv Rev.* (2006).**584**:67–86.

Patil, V., Malvamka, R.B., Sastry, M., *Langmuir*. (1999).**15**:81-97.
Pernodet, N., Fang, X., Sun, Y., Bakhtina, A., Ramakrishnan, A., Sokolov, J., Ulman, A., Rafailovich, M. *Small.* (2006), **2**, 766.

Peters, T. Serum Albumin. *Adv. Prot. Chem.* (1985),**37**:161–245.

Prato, M., Kostarelos, K., Bianco, A. Functionalized carbon nanotubes in drug design and discovery. *Acc Chem Res*. (2008).**41**:60–80.

Putnam, D. Polymers for gene delivery across length scales. *Nat Mater*. (2006),**5**:439–451.

Ramya, T. N. C., Surolia, N. N., Surolia, A. 15-Deoxyspergualin modulates *Plasmodium falciparum* heat shock protein function. *Biochem. Biophys. Res. Commun*. (2006), **348**: 585-592.

Rawat, M., Singh, D., Saraf, S. Nanocarriers: promising vehicle for bioactive drugs. *Biol Pharm Bull*. (2006),**29**:1790–1798.

Roco, M. C. Nanoparticles and Nanotechnology Research. *Journal of Nanoparticle Research.* (1999),**1**:1-6.

Rüdiger, S., Germeroth, L., Schneider-Mergener, J., and Bukau, B. Substrate specificity of the DnaK chaperone determined by screening cellulose-bound peptide libraries. *EMBO J*. (1997), **16**: 1501-1507.

Ryan, J.A., Overton, K.W., Speight, M.E. Cellular uptake of gold nanoparticles passivated with BSA-SV40 large t antigen conjugates. *Anal Chem,* (2007), **79**: 91–99.

Sahoo, S.K., Parveen, S., Panda, J.J. The present and future of nanotechnology in human health care. *Nanomedicine*. (2007), **3**:20–31.

Sapsford, K.E., Berti, L., Medintz, I.L. Materials for fluorescence resonance energy transfer analysis: beyond traditional donor–acceptor combinations, *Angew Chem., Int. Ed*. (2006),**45**:4562–4589.

Sarangi, S.N., Hussain, A.M.P., Sahu, S.N. Strong UV absorption and emission from L-cysteine capped monodispersed gold nanoparticles. *Applied physics Letter.* (2009). **95**:103-109.

Sarre, S., Van-Belle K., Smolders, I., Krieken, G., Michotte, Y. The use of microdialysis for the determination of plasma protein binding of drugs. *J. Pharm. Biomed. Anal.* (1992). **10:**735–739.

Sato, K., Hosokawa, K., Maeda, M. Rapid aggregation of gold nanoparticles induced by non-cross-linking DNA hybridization. *J Am Chem Soc*, (2003), **125**:8102–8113.

Sershen, S.,West, J. Implantable, polymeric system for modulated drug delivery. *Adv, Drug Del.Rev*. (2002).**54**(9):1225-1235.

Shang, L., Wang, Y., Jiang, J., Dong, S. pH-Dependent protein conformational changes in albumin: Gold nanoparticle bioconjugates: A spectroscopic study. *Langmuir.* (2007). **23**: 2714-2721.

Shang, W., Nuffer, J.H., Dordick, J.S., Siegel, R.W. Unfolding of ribonuclease A on silica nanoparticle surfaces. *Nano Lett. (*2007),**7**:1991-1995.

Shi, N.W., Kam, O., Connell, M., Wisdom, J.A., Dai, H. Carbon nanotubes as multifunctional biological transporters and near-infrared agents for selective cancer cell destruction .*Proc.Natl Acad.Sci*. *USA*. (2005),**102** (33): 11600-11603.

Shonhai, A., Stephens, L., Blatch, G. heterologous expression of plasmodial proteins for structural studies and functional annotations. *malaria journal*, (2008).

Shonhai A. plasmodial heat shock proteins: targets for chemotherapy, *immunol med microbiology*, (2010). 61-74.

Shonhai, A., Boshoff, A., Blatch, G.L. Plasmodium falciparum heat shock protein 70 is able to suppress the thermosensitivity of an Escherichia coli DnaK mutant strain. *Mol Genet Genomics*. (2005). **4**: 70–78.

Shu, X. Z., Zhu, K. J. *Int. J. Pharm.* (1999).**1**:*201*, 51.
Silvia, H., De Paoli, L., Park, J.J., Curt, M., Pristinski, D., Becker, M., Karim, A., Douglas, F.G. Interaction of gold nanoparticles with common human blood proteins. *ACSNANO*. (2010). **4**: 365-379.

Sugio, S. Crystal Structure of Human Serum Albumin at 2.5 A Resolution. *Prot. Eng*. (1999).**12**: 439–446.

Suzuki, K., Sawa, Y., Kagisaki, K. Reduction in myocardial apoptosis associated with over expression of heat shock protein 70. *Basic Res Cardiol*. (2000), **95**:397– 403.

Szabo, A., Langer, T., Schröder, H., Flanagan, J., Bukau, B., Hartl, F.U. The ATP hydrolysis-dependent reaction cycle of the *Escherichia coli* Hsp70 system—DnaK, DnaJ and GrpE. Proc. *Natl. Acad. Sci. U.S.A*. (1994). **91**:10345–10349.

Tang, K., Chen, D., Liu, Y., Shen, G., Zheng, H., Qian, Y. “Shape-controlled synthesis of copper sulfide nanocrystals via a soft solution route,” *Journal of Crystal Growth*, (2004).**263**:232–236.

Thomas, C.E., Ehrhardt, A., Kay, M.A. Progress and problems with the use of viral vectors for gene therapy. *Nat Rev Genet.* (2003),**4**:346–58.

Tkachenko, A. G., H. Xie., Y. Liu., Coleman,D., Ryan, J., Glomm, W.R., Shipton, M.K., Franzen, S., Feldheim, D.L. Bioconjugate. *Chem*. (2004), **15**:482.

Turkevich J. Colloidal Gold, *gold bulletin*. (1985), **18**:3.

Turkevich, J., Stevenson, P. C., Hillier, J. Discuss*. Faraday Soc.* (1951) **11**:55–75.

Vertegel, A.A., Siegel, R.W., Dordick, J.S. Silica nanoparticle size influences the structure and enzymatic activity of adsorbed lysozyme. *Langmuir.* (2004), **20**:6800-6807.

Vroman, L., Adams, A.L., Fischer, G.C., Munoz, P.C. Interaction of highmolecular weight kininogen, factorXII, andfibrinogen inplasma at interfaces. *Blood.* (1980), **55**:156–159.

Wang, J., Xu, D., Kawde, A.N., Polsky, R. *Anal. Chem.* (2001) **73**:55-76.
Wang, J., Xu, D., Polsky, R. *J. Am. Chem. Soc*. (2002), **124:**42-48.

Wang, J., Polsky, R., Xu, D. Interaction of gold nanoparticles with biomolecules. *Langmuir*. (2001), **17**:39-57.

Wang, J., Xu, D., Kawde, A.N., Polsky, R. Size dependent cytotoxicity of gold nanoparticles. *Anal. Chem*. (2001), **73:**55-76.

Wiethoff, C.M., Middaugh, C.R. Barriers to nonviral gene delivery. *J. Pharm. Sci*. (2003), **92:**203–217.

Wu, X., Narsimhan, G. Effect of surface concentration on secondary and tertiary conformational changes of lysozyme adsorbed on silica nanoparticles. *Biochim. Biophys. Acta.* (2008),**1784***:*1694-1701.

Xiao, Y., Pavlov, V., Levine, S., Niazov, T., Markovitch, G., Willner, I. Catalytic growth of Au nanoparticles by NAD(P)H cofactors: optical sensors for NAD(P)+. (2004), **58**:3–7.

Yang, S., Zhang, T., Zhang, L., Wang, S., Yang, Z., Ding, B. Colloids Surf A. *Physicochem Eng Asp.* (2007),**296**:37– 44.

Zakrzewski, K. Cross-linkages in human serum albumin polymerized by gamma irradiation in solution. *Rad. Res.* (1973), **53**:124–133.

Zhu, M. Apparatus Analyses. *Beijing*: *Higher EducationPress*. (2000).

Zsigmondy, R. Colloidal ultramicroscope. *J. alaxader, trans., wiley new York.* (1909).

Appendix A

General experimental procedures

A.1. Sodium dodecyl polyacrylamide gel electrophoresis (SDS-PAGE)

The resolution of proteins was carried out using 12 % acrylamide resolving gel using the concept of staggered buffering system (Laemmli, 1970). The electrophoresis was conducted using the Bio-Rad Mini protein 3 electrophoresis system (Biorad, U.S.A). Preparation of resolving and stacking buffers was carried out as shown (Table A1). Gels were allowed to stand for 30 minutes for the polymerisation to complete. They were then transferred into the electrophoresis tank and electrophoresis buffer (25 mM Tris, pH 8.3 250 mM glycine and 0.1 % (w/v) SDS) was added.

In order to prepare protein samples for analysis, they were mixed with SDS sample buffer (0.25 % Coomasie Brilliant blue (R250); 2 % SDS; 10 % glycerol (v/v); 100 mM tris; 1 % mercaptoethanol) in a ratio of 1 : 1 and boiled for 5 minutes at 95°C. The protein samples were loaded into gel wells. Bio-Rad premixed molecular weight markers were also loaded. The electrophoresis was allowed to run for at least 1 hour 30 minutes at 120 volts.

Table A.1 Solutions for making a 5 % stacking gel and a 12 % resolving gel for SDS-PAGE

Reagent (ml)	5 % stacking gel	12 % resolving gel
Distilled water	4.1	4.9
30 % polyacrylamide	1.0	6.0
1.5 M Tris (pH 8.8)	-	3.8
1.0 M Tris (pH 6.8)	0.75	-
10 % Ammonium persulphate	0.06	0.15
TEMED	0.006	0.006
Total volume	6 ml	15 ml

Table A2 Phosphate saline buffer

Ml	300	500
1.37 mM Nacl	2.4	4
2.7 mM kcl	0.06	0.1
4.3 mM Na_2HPO_4	0.432	0.72
1.4 mM KH_2PO_4	0.072	0.12

pH adjusted using 0.1M HCL for acidic and 0.1M NAOH for basic

Table A3 SDS-PAGE running buffer

ml	2000 (1x)	5000 (1x)	1000 (5x)
Tris	6.05	15.125	15.125
Glycine	28.8	72	72
SDS	2.0	5	5

Table A4 SDS-PAGE sample buffer

Ml	8.0	16	48
Deionized water	3.8	7.6	22.8
0.5 M tris pH 6.8	1.0	2.0	6
Glycerol	0.8	1.6	4.8
10% SDS	1.6	3.2	9.6
2 Mercaptoethanol	0.4	0.8	2.4
1% bromophenol blue	0.4	0.8	2.4

A.2. Visible and Ultraviolet spectroscopy

Wavelength is the distance between adjacent peaks (or troughs) and is designated in meters, centimeters and nanometers. Visible wavelength covers a range from approximately 400nm – 800nm and the longest wavelength is red and the shortest is violet in colour. When white light passes through or is reflected by a coloured substance, a characteristic portion of the mixed wavelengths is absorbed and the remaining light assumes the complementary colour to the absorbed wavelength. Complementary colours are diametrically opposite each other.

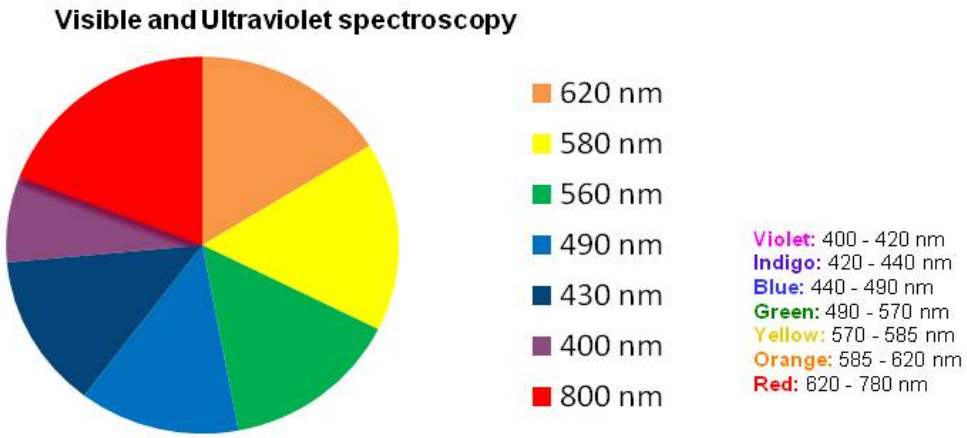

Figure A1 ultraviolet visible spectroscopy principle
Diagrammatic representation of Visible and Ultraviolet spectroscopy and complementary colours are diagrammatically opposite each other.

Appendix B

Supplementary Data

Table B.1 AuNPs features resulted from varied synthesis conditions

Cysteine [ ]	$AuCl_3$ [ ]	$NaBH_4$ [ ]	Wavelength peak (nm)	Size/diameter (nm)	Reaction time	Reference
1 mM	0.05 M	0.01 M	361	± 3	2 hours	Sarangi *et al*., 2009
2 mM	0.05 M	0.01 M	363	± 2	30 mins	Sarangi *et al*., 2009
3 mM	0.05 M	0.01 M	377	± 1	2 hours	Sarangi *et al*., 2009
4 mM	0.05 M	0.01 M	375	± 1	30 mins	Sarangi *et al*., 2009
33 mM	0.1 M	0.1 M	535	± 35	2 hours	Horovitz *et al*., 2007
33 mM	0.1 M	0.1 M	530	± 40	30 mins	Chili *et al*., 2008

[ ]: Concentration
(nm): Nanometer
±: Plus or minus
Mins: minutes

Appendix C

Special reagents and chemicals

Table C.1 Special chemical reagents and kits

Name of reagent	Vendor/Supplier
$AuCl_3$	Sigma Aldrich
Bovine serum albumin	Sigma Aldrich
Bromophenol blue	Sigma Aldrich
Citrate synthase	Sigma Aldrich
Coomasie brilliant blue	Amarsham, U.S.A
Glycial acetic acid	Merck, Germany
Glycerol	Merck, Germany
Glycine	Sigma, U.S.A
HEPES	Amarsham, U.S.A
Human heat shock protein70	Sigma, U.S.A
Methanol	Merck, Germany
Sodium chloride	Merck, Germany
TEMED	Sigma, U.S.A
Tryptone	Oxoid, U.K
Yeast	Oxoid, U.K